# Structure-Based Design of Novel 2-Amino-6-phenyl-pyrimido[5′,4′:5,6]pyrimido[1,2-*a*]benzimidazol-5(6*H*)-ones as Potent and Orally Active Inhibitors of Lymphocyte Specific Kinase (Lck): Synthesis, SAR, and In Vivo Anti-Inflammatory Activity

Matthew W. Martin,*[,†] John Newcomb,[‡] Joseph J. Nunes,[†] Christina Boucher,[‡] Lilly Chai,[‡] Linda F. Epstein,[§] Theodore Faust,[‡] Sylvia Flores,[#] Paul Gallant,[‡] Anu Gore,[⊥] Yan Gu,[§] Faye Hsieh,[||] Xin Huang,[§] Joseph L. Kim,[§] Scot Middleton,[#] Kurt Morgenstern,[§] Antonio Oliveira-dos-Santos,[‡] Vinod F. Patel,[†] David Powers,[○] Paul Rose,[§] Yanyan Tudor,[□] Susan M. Turci,[‡] Andrew A. Welcher,[□] Debra Zack,[#] Huilin Zhao,[§] Li Zhu,[#] Xiaotian Zhu,[§] Chiara Ghiron,[△] Monika Ermann,[△] David Johnston,[△] and Carl-Gustaf Pierre Saluste[△]

*Department of Medicinal Chemistry, Department of HTS and Molecular Pharmacology, and Department of Molecular Structure, Amgen Inc., One Kendall Square, Building 1000, Cambridge, Massachusetts 02139, Department of Inflammation, Department of Pharmaceutics, Department of Pharmacokinetics and Drug Metabolism, Department of HTS and Molecular Pharmacology, and Department of Molecular Sciences, Amgen Inc., One Amgen Center Drive, Thousand Oaks, California 91320, and Evotec OAI, 151 Milton Park, Abingdon, Oxon OX14 4SD, United Kingdom*

*Received September 4, 2007*

Lck, or lymphocyte specific kinase, is a cytoplasmic tyrosine kinase of the Src family expressed in T-cells and NK cells. Genetic evidence from knockout mice and human mutations demonstrates that Lck kinase activity is critical for T-cell receptor-mediated signaling, leading to normal T-cell development and activation. A small molecule inhibitor of Lck is expected to be useful in the treatment of T-cell-mediated autoimmune and inflammatory disorders and/or organ transplant rejection. In this paper, we describe the structure-guided design, synthesis, structure–activity relationships, and pharmacological characterization of 2-amino-6-phenylpyrimido[5′,4′:5,6]pyrimido[1,2-*a*]benzimidazol-5(6*H*)-ones, a new class of compounds that are potent inhibitors of Lck. The most promising compound of this series, 6-(2,6-dimethylphenyl)-2-((4-(4-methyl-1-piperazinyl)phenyl)amino)pyrimido[5′,4′:5,6]pyrimido-[1,2-*a*]benzimidazol-5(6*H*)-one (**25**), exhibits potent inhibition of Lck kinase activity. This activity translates into inhibition of in vitro cell-based assays and in vivo models of T-cell activation and arthritis, respectively.

## Introduction

T-cells play a pivotal role in the adaptive immune response by acting either as potentiators (CD4+ T-helper cells) or effectors (CD8+ cytolytic T-effector cells) of immune reactions. The immune specificity of a particular T-cell is determined by the T-cell receptor (TCR[a]) for antigen, or CD3 complex, expressed on its surface.[1] Signaling pathways used by the TCR have been an intense area of research toward the discovery of novel immunosuppressive agents. The goal of this research is the development of improved therapies for graft rejection and T-cell-mediated autoimmune disease. A number of protein kinases have been shown to be important for TCR signal transduction. The Src family of cytoplasmic tyrosine kinases consists of nine members: Src, Lck, Fyn, Lyn, Hck, Fgr, Blk, Yes, and Yrk.[2,3] Among the Src family, Lck and Fyn have been shown to have important roles in TCR signal transduction.[4–6] TCR signals initiated by Lck lead to gene regulation events resulting in cytokine release, proliferation, and survival of antigen specific T-cells. Lck knockout mice and patients with Lck mutations effecting protein expression and/or catalytic activity display common phenotypes involving defects in T-cell maturation and signaling.[7–12] Taken together, these findings suggest that a small molecule inhibitor of Lck kinase activity might be a useful immunosuppressive agent for the treatment of graft rejection and/or T-cell-mediated autoimmune diseases.

As part of our ongoing efforts to identify small molecule inhibitors of Lck for the development of new therapeutic agents, we recently disclosed a number of promising chemical series.[13] In addition, several other groups have previously illustrated the synthesis and characterization of Lck- or Src-family kinase inhibitors.[14–19] Potent and bioavailable Lck/Src inhibitors have also been demonstrated to have efficacy in several in vivo models of T-cell-dependent immune responses.[13a,b,17f,18d,20]

Screening of our in-house kinase preferred collection identified aminobenzimidazole triazines, such as *N*-phenyl-1-(4-(3,4,5-trimethoxyphenylamino)-1,3,5-triazin-2-yl)-1*H*-benzo[*d*]imidazol-2-amine and *N*-(2,6-dimethylphenyl)-1-(4-(3,4,5-trimethoxyphenylamino)-1,3,5-triazin-2-yl)-1*H*-benzo[*d*]imidazol-2-amine (compounds **1** and **2**, respectively, Figure 1), as potent inhibitors of Lck. Unfortunately, these compounds were nonselective kinase inhibitors, exhibiting, for example, equal, low-nanomolar potency against KDR. A cocrystal structure of **1** bound to Lck revealed key interactions in the ATP-binding pocket (Figure 2). Binding to Lck is anchored by three hydrogen-bond interactions between the aminotriazine moiety of compound **1** and the kinase linker region: Met319 H-bonds

* To whom correspondence should be addressed: Tel.: 617-444-5013. Fax: 617-621-3908. E-mail: matmarti@amgen.com.
† Department of Medicinal Chemistry.
‡ Department of HTS and Molecular Pharmacology, Cambridge, MA.
§ Department of Molecular Structure.
⊥ Department of Pharmaceutics.
|| Department of Pharmacokinetics and Drug Metabolism.
# Department of Inflammation.
○ Department of HTS and Molecular Pharmacology, Thousand Oaks, CA.
□ Department of Molecular Sciences.
△ Evotec OAI.

[a] Abbreviations; Lck, lymphocyte specific kinase; TCR, T-cell receptor; IL-2, interleukin 2; PTK, protein tyrosine kinase; VEGFR-2, vascular endothelial growth factor receptor-2; KDR, kinase insert domain receptor; MAPK, mitogen-activated protein kinase; huMLR, human mixed lymphocyte reaction.

10.1021/jm701095m CCC: $40.75 
Published on Web 02/16/2008

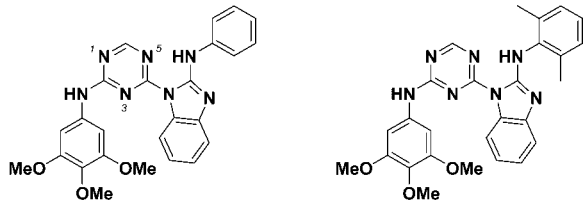


**Figure 1.** Structure and activity of aminobenzimidazole triazines **1** and **2**.

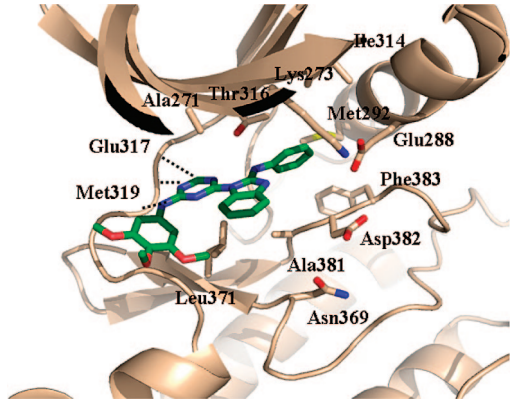


**Figure 2.** X-ray cocrystal structure aminobenzimidazole triazine **1** bound to Lck.

**Table 1.** Sequence Comparison at Gatekeeper Residue

| kinase | Lck | KDR | p38α |
|---|---|---|---|
| gatekeeper residue | Thr316 | Val916 | Thr106 |

through the main chain NH and carbonyl to the triazine N3 (2.8 Å) and 2-amino NH (2.8 Å), respectively, while the main chain carbonyl of Glu317 H-bonds to the CH in the 4-position of the triazines (3.1 Å).[21] This binding mode directs the aniline substituent of the benzimidazole core into the hydrophobic pocket adjoining the ATP-binding site in Lck. Interestingly, the cocrystal structure revealed that the N5-triazine and 2-anilinobenzimidazole nitrogens were only 4.3 and 3.8 Å, respectively, away from the $\gamma$-OH of the gatekeeper residue, Thr316.

We sought to exploit the proximity and hydrogen-bonding capacity of the gatekeeper threonine in Lck and take advantage of sequence differences among structurally related kinases in and around the ATP-binding pocket (Table 1). In particular, we designed the 2-amino-6-phenylpyrimido[5′,4′:5,6]pyrimido[1,2-*a*]benzimidazol-5(6*H*)-ones, exemplified by compound **3** (Figure 3), which possess a carbonyl oxygen that is well-positioned to accept a hydrogen bond from the $\gamma$-OH of Thr316 in the ATP-binding site of Lck (donor–acceptor distance is 2.4 Å, with an acceptor–donor−hydrogen angle of about 20 degrees).[22] We hypothesized that such a new interaction would increase selectivity over kinases with nonthreonine gatekeeper residues, namely, KDR.[23] Herein we describe the synthesis, structure–activity relationships, and pharmacological characterization of 2-amino-6-phenylpyrimido[5′,4′:5,6]pyrimido[1,2-*a*]benzimidazol-5(6*H*)-ones, a new class of compounds with potent inhibition of Lck. Lead optimization led to the discovery of compounds

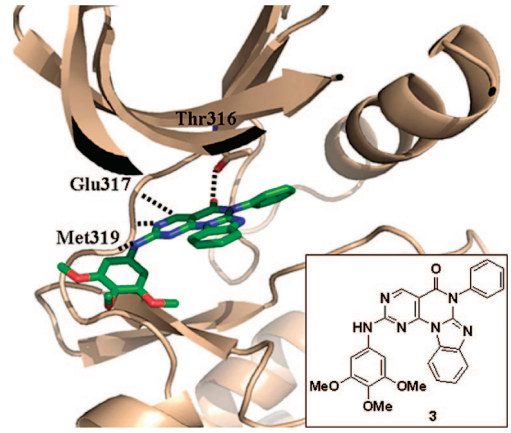


**Figure 3.** Model of 2-amino-6-phenylpyrimido[5′,4′:5,6]pyrimido[1,2-*a*]benzimidazol-5(6*H*)-one **3** bound to Lck.

**Scheme 1.** Retrosynthetic Analysis of 2-Amino-6-phenylpyrimido[5′,4′:5,6]pyrimido[1,2-*a*]benzimidazol-5(6*H*)-ones

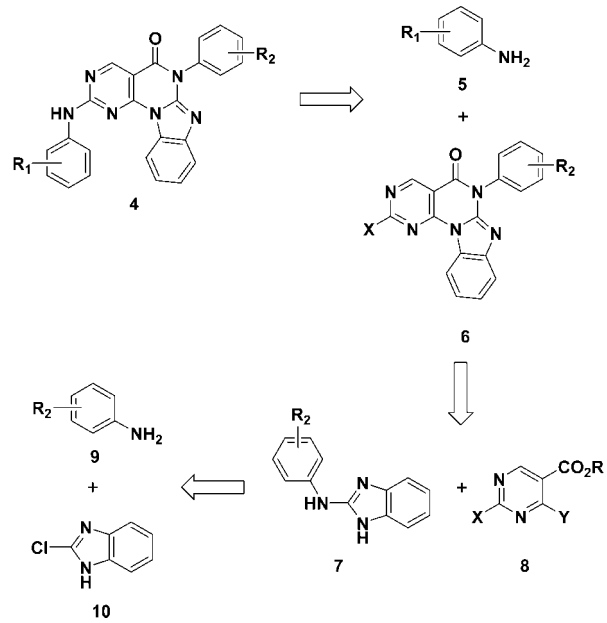


which demonstrated inhibition of T-cell activation in in vitro and in vivo biological assays as well as in models of rheumatoid arthritis.

## Chemistry

Our strategy for the construction of the 2-amino-6-phenylpyrimido[5′,4′:5,6]pyrimido[1,2-*a*]benzimidazol-5(6*H*)-ones described in this paper is outlined in the retrosynthetic analysis shown in Scheme 1. In this approach, we envisioned accessing tetracycles **4** via the nucleophilic addition of anilines **5** to 2-substituted tetracyclic pyrimidines **6** (X = Cl or $SO_2Me$). Tetracyclic pyrimidines **6**, in turn, would be derived in two steps via nucleophilic attack of anilines **9** on 2-chlorobenzimidazole (**10**) followed by addition of the resulting 2-aminobenzimidazoles **7** to 2,4-disubstituted pyrimidine **8** (X = Cl or SMe, Y = Cl). This concise route would allow for rapid analoging as each variation could be introduced by simply employing the desired aniline.

The anilines required for the syntheses of the tetracycles shown in Tables 1 and 2 were either obtained from commercial sources or prepared via one of the methods shown in Scheme

**Scheme 2.** Synthesis of Aniline Side Chains[a]

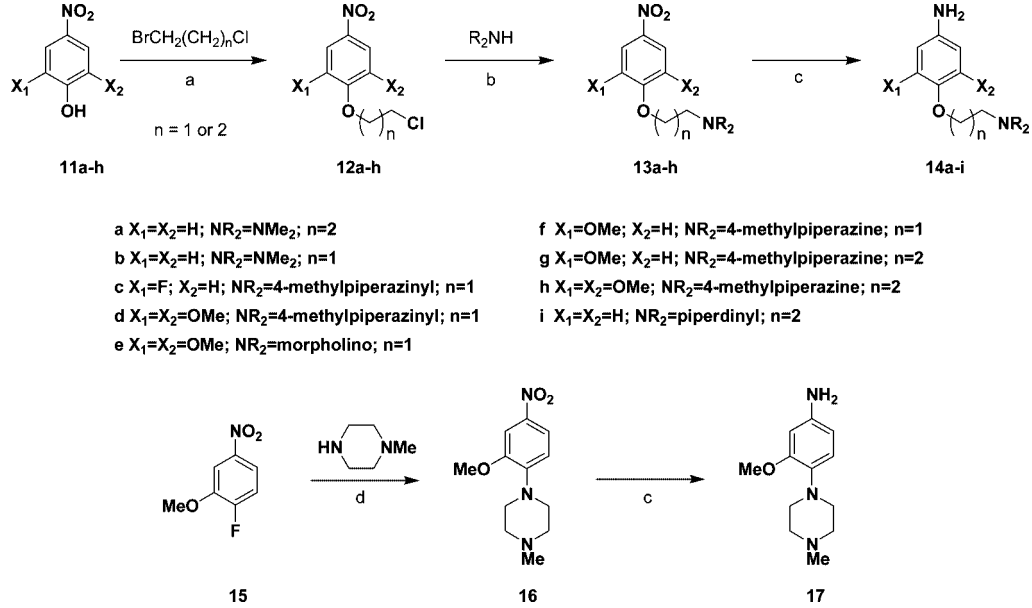


[a] Reagents and conditions: (a) $K_2CO_3$, MeCN, reflux; (b) $K_2CO_3$, MeCN, 80 ºC, 57% (two steps); (c) $H_2$, 10% Pd/C, EtOH, rt, 16 h, 100%; (d) 100 ºC, 49%.

**Scheme 3.** Synthesis of 2-Amino-6-phenylpyrimido[5′,4′:5,6]pyrimido[1,2-*a*]benzimidazol-5(6*H*)-ones[a]

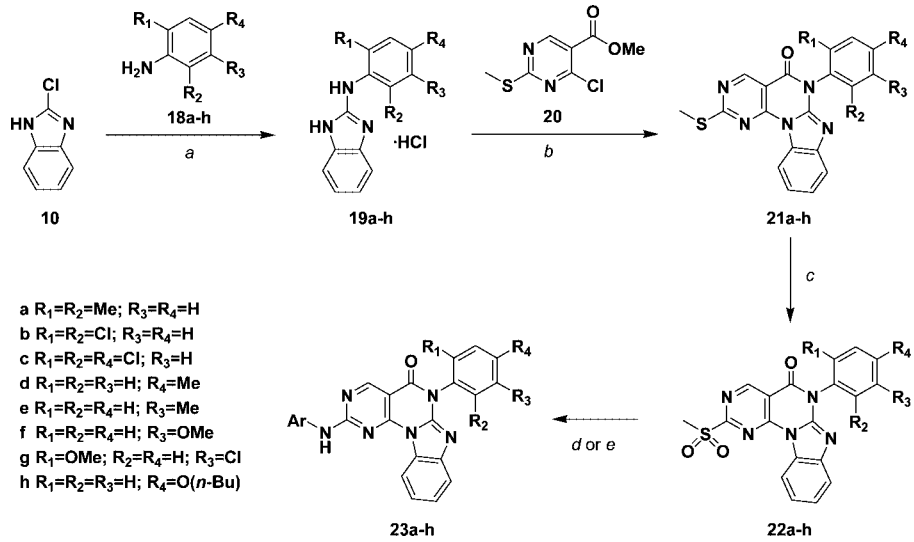


[a] Reagents and conditions: (a) reflux, 24 h, 79%; (b) $(i\text{-Pr})_2$NEt, toluene, 110 °C, 3 d, 60 %; (c) *m*-CPBA, $CH_2Cl_2$, rt, 20 h, 97%; (d) $ArNH_2$, *i*-PrOH, $CF_3CO_2H$, 80 °C, 5−16 h, 93%; (e) $ArNH_2$, *i*-PrOH, 80 °C, 5 h, 58%.

2. The 4-alkoxy-substituted anilines **14** were synthesized from the corresponding nitrophenols **11** via an alkylation with either 1-bromo-2-chloroethane or 1-bromo-3-chloropropane. The resulting alkylchloride **12** then underwent nucleophilic displacement with the desired amine (dimethylamine, morpholine, or *N*-methylpiperazine) to afford *p*-alkoxynitrophenyl derivative **13**. Catalytic hydrogenation with palladium on carbon afforded the corresponding aniline **14**. For 3-methoxy-4-(4-methylpiperazin-1-yl)aniline (**17**), 1-fluoro-2-methoxy-4-nitrobenzene (**15**) was heated with *N*-methylpiperazine to afford 1-(2-methoxy-4-nitrophenyl)-4-methylpiperazine (**16**). Reduction via catalytic hydrogenation with palladium on carbon afforded the desired aniline **17**.

The synthesis of the 2-amino-6-phenylpyrimido[5′,4′:5,6]pyrimido[1,2-*a*]benzimidazol-5(6*H*)-ones is shown in Scheme 3. A solution of 2-chlorobenzimidazole (**10**) and the desired aniline **18** were refluxed overnight to afford the desired 2-aminobenzimidazole **19** as the hydrochloride salt. Heating of **19** with ethyl 4-chloro-2-methylthiopyrimidine-5-carboxylate (**20**) in the presence of diisopropylethylamine afforded tetracycle **21**. Activation of the sulfide via oxidation with *m*-chloroperoxybenzoic acid afforded sulfone **22**, which could be displaced with a variety of anilines to afford a series of tetracyclic pyrimidine derivatives **23**. In general, heating a solution of the sulfone and aniline in isopropanol with or without trifluoroacetic acid was used.[24]

## Results and Discussion

**Structure–Activity Relationships (SAR).** All compounds were screened for inhibitory activity against Lck in a homogeneous time-resolved fluorescent (HTRF) kinase assay. Selected compounds were tested for cellular activity by measuring the inhibition of T-cell receptor-induced IL-2 production in human T-cells as well as for the inhibition of T-cell activation in a human mixed lymphocyte reaction (huMLR).

**Table 2.** SAR: Variations of the Aniline Side Chain[a]

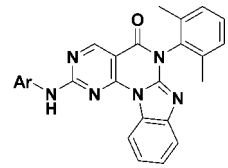

| | | IC$_{50}$ (μM) | | | | | | | |
|---|---|---|---|---|---|---|---|---|---|
| | Ar | Lck | Src | p38α | KDR | IL-2[b] | huMLR[c] | clog$P$[d] | SIF sol.[e] (μg/mL) |
| **24** | 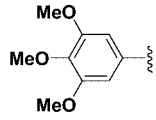 | 0.027 | 0.21 | >10 | 1.9 | 0.97 | 0.47 | 5.6 | 15 |
| **25** | 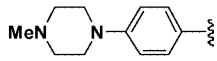 | 0.007 | 0.12 | >10 | 5.1 | 0.46 | 0.047 | 5.0 | 153 |
| **26** | 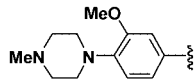 | 0.005 | 0.10 | 7.5 | 3.6 | 0.43 | 0.051 | 5.4 | >200 |
| **27** | 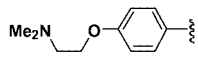 | 0.028 | 0.44 | >10 | 6.6 | -- | 0.084 | 5.2 | -- |
| **28** | 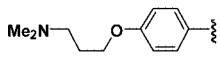 | 0.020 | 0.36 | >10 | 4.2 | 1.1 | 0.10 | 5.5 | 155 |
| **29** | 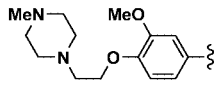 | 0.019 | 0.24 | >10 | 5.5 | 16 | 0.15 | 4.6 | -- |
| **30** | 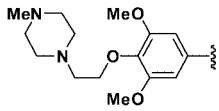 | 0.006 | 0.077 | >10 | 3.3 | 0.61 | 0.29 | 4.7 | >200 |
| **31** | 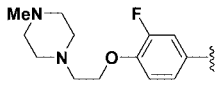 | 0.023 | 0.16 | >10 | 7.4 | 2.7 | 0.51 | 4.9 | -- |
| **32** | 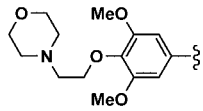 | 0.010 | 0.044 | >10 | 1.7 | 0.36 | 0.18 | 4.9 | 18 |
| **33** | 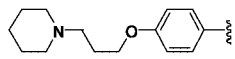 | 0.012 | 0.16 | 4.3 | 5.1 | 3.6 | 0.37 | 6.8 | 101 |
| **34** | 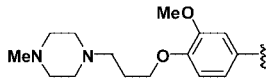 | 0.012 | 0.18 | >10 | 5.0 | 1.5 | 0.14 | 5.0 | >200 |
| **35** | 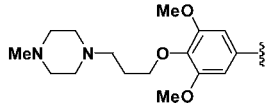 | 0.006 | 0.07 | >10 | 4.0 | 0.19 | 0.080 | 5.1 | -- |

[a] IC$_{50}$values are the means of two or more separate determinations, in duplicate; standard deviations were generally within ±30% of the mean. [b] IL-2: anti-CD3/CD28-induced T-cell IL-2 secretion assay. [c] huMLR: human mixed lymphocyte reaction. [d] Determined using ACD Labs 8.0. [e] SIF sol.: simulated intestinal fluid solubility assay.

For purposes of determining kinase selectivity, the compounds were also tested against related kinases Src, p38α, and KDR. Mitogen-activated protein kinase (MAPK) p38α is a serine/threonine kinase and a key signaling protein for multiple processes that are activated in inflammation, such as the biosynthesis of pro-inflammatory cytokines TNFα and IL-1$\beta$.[25] The vascular endothelial growth factor receptor-2 (VEGFR-2; also referred to as the kinase insert domain receptor or KDR)

is a receptor protein tyrosine kinase involved in angiogenesis, the formation of new vasculature from existing blood vessels. Aberrant angiogenesis has been associated with a variety of disorders including rheumatoid arthritis and cancer.[26] Thus, selectivity over p38α and KDR is important for proof of concept studies.

Aminobenzimidazole triazines **1** and **2** exhibited excellent enzyme potency on Lck (6 and 1 nM, respectively) but lacked selectivity over KDR (7 and 4 nM). Our initial work focused on the hypothesis that introducing a carbonyl group to engage the Thr316 γ-OH in Lck (and clash with the Val916 γ-methyl in KDR) would provide compounds with improved selectivity while maintaining Lck potency. As shown in Table 2, compound **24**, a closely related derivative of **3** (the inhibitor modeled to examine the feasibility of this idea), served as a promising starting point. While **24** did exhibit a 30-fold loss in potency against Lck (relative to **2**), we were encouraged by the 1000-fold loss in potency against KDR. In addition, this change was coupled with a surprising >100-fold loss in potency against p38α (which also possesses a Thr gatekeeper) relative to compound **2** (p38α $IC_{50}$ = 78 nM). With this promising result in hand, we set out to explore whether altering the aniline side chain could increase Lck potency while maintaining the high levels of selectivity.

The crystal structure of compound **1** bound to Lck (Figure 2) as well as our model of **3** (Figure 3) revealed that substituents on the aniline at C2 should be projected toward solvent. We reasoned that the introduction of an ionizable group at the *para*-position of this ring might improve cell permeability and potency, as well as oral bioavailability. In addition, a slight boost in enzyme potency might be gained via interactions with residues along the solvent front.[27] As shown in Table 2, alterations to the aniline side chain were well-tolerated, with all variations affording compounds that were potent inhibitors of Lck and many exhibiting a marked improvement in solubility (>10-fold increase relative to **24**). The main area of differentiation between these compounds was their cellular activity. Replacing the methoxy groups with a tertiary amine such as the *N*-methylpiperazine in **25** and **26** resulted in compounds with a 3- to 5-fold increase in enzyme activity as well as a 10-fold increase in cell potency (huMLR data; increased potency presumably due to improved solubility and/or cell permeability). Selectivity over KDR increased to well over 500-fold, with >100-fold selectivity observed over p38α. Replacement of the *N*-methylpiperazine with 2-(dimethylamino)ethoxy or 2-(dimethylamino)propoxy groups (**27** and **28**) also improved cell potency in the huMLR by 3- to 4-fold, though the potency remained the same (relative to **24**). Replacing the dimethylamino group on the alkoxy side chain with a cyclic amine, such as piperidine (compound **33**), had little impact on potency or selectivity.

We also investigated the impact of combining substituted anilines with variations on the alkoxy side chain. 3-Fluoro-substituted aniline (**31**) showed a slight improvement in KDR but with similar levels of Lck enzyme and cell potency relative to **24**. 3,5-Dimethoxy derivatives **30** and **35** showed improved enzyme and cellular potency while maintaining excellent selectivity over KDR and p38α (>500-fold for both). Replacing the *N*-methylpiperazine with a morpholine (**32**) had little impact on enzyme and cell potency, but a slight decrease in selectivity over KDR (relative to compound **30**) was observed. Overall, changes to the aniline side chain had minimal impact in terms of potency and selectivity. This is consistent with previously observed results in related series of compounds[13a] and is consistent with the aniline side chain pointing toward the solvent front and having minimal interactions with the protein. Because of its excellent enzyme and cellular potency and selectivity profile, coupled with its ease of synthesis (4-(4-methylpiperazin-1-yl)aniline is commercially available), we chose to conduct subsequent SAR studies around **25**.

**Table 3.** SAR:Variations of the 6-Aryl Group[a]

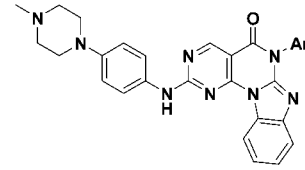

| | Ar | $IC_{50}$ (μM) Lck | Src | KDR | p38α | huMLR[b] |
|---|---|---|---|---|---|---|
| **25** |  | 0.007 | 0.12 | 5.1 | >10 | 0.047 |
| **36** |  | 0.010 | 0.049 | 0.53 | -- | 1.1 |
| **37** |  | 0.008 | 0.035 | 0.48 | >10 | 0.14 |
| **38** |  | 0.35 | 1.7 | >25 | -- | -- |
| **39** |  | 0.096 | 1.0 | >25 | -- | -- |
| **40** | 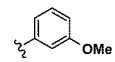 | 0.19 | 1.9 | 8.3 | -- | -- |
| **41** | 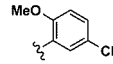 | 0.023 | 1.4 | >25 | -- | 1.0 |
| **42** | 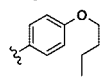 | 4.6 | 8.3 | >25 | -- | -- |

[a] $IC_{50}$ values are the means of two or more separate determinations, in duplicate; standard deviations were generally within ±30% of the mean. [b] huMLR: human mixed lymphocyte reaction.

We also explored the effect of varying the substitution on the aniline pointing into the kinase specificity pocket. As shown in Table 3, 2,6-disubstitution affords the most potent compounds (**25**, **36**, and **37**). This is consistent with observations from previous groups,[16a,17a] as well as our own in-house studies,[13a] which demonstrate that a 2,6-disubstituted aniline is the optimal substitution pattern. To avoid steric interactions, the two *ortho*-groups position the aniline orthogonal to the tetracyclic core, allowing it to easily fill the hydrophobic pocket. Compounds with monosubstitution in either the *para*- (**38**) or *meta*-positions (**39** and **40**) showed reduced potency (15- to 50-fold) relative to **25**. The loss of enzyme potency was less significant (3-fold) when the compound contained a 2,5-disubstituted aniline (**41**), but this was combined with a 20-fold loss in cell potency. Introduction of larger groups, such as the *p*-butoxy in **42**, resulted in an almost complete loss of potency against Lck (>4 μM). Because none of these alterations offered any improvement, we chose to further explore the properties of **25**.

**Structural Confirmation.** To confirm the binding elements responsible for the observed potency and selectivity of this series of compounds, we obtained a cocrystal structure of Lck with 2-amino-6-phenylpyrimido[5′,4′:5,6]pyrimido[1,2-*a*]benzimidazol-5(6*H*)-one **25** (Figure 4). Consistent with findings from our previous work,[13a] the aniline side chain of **25** extends to the mouth of the ATP-binding pocket, with the *N*-methylpiperazine moiety fully exposed to solvent. The 6-phenyl group is rotated 80 degrees from the tetracyclic plane due to the presence of

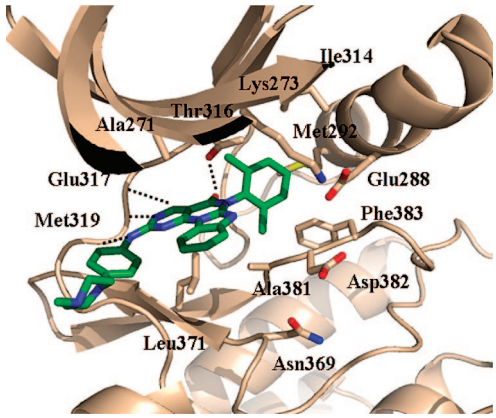


**Figure 4.** X-ray cocrystal structure of 2-amino-6-phenylpyrimido[5′,4′:5,6]pyrimido[1,2-*a*]benzimidazol-5(6*H*)-one **25** bound to Lck.

the 2,6-substituents, which appropriately orients the aromatic ring to enter the deep hydrophobic pocket adjoining the ATP-binding site. Hydrogen bond interactions between the inhibitor **25** and the linker region of the protein are similar to those observed with compound **1** and described above. Additionally, a novel, fourth hydrogen bond is observed. As we hypothesized, the carbonyl of the tetracycle **25** accepts a hydrogen bond from the $\gamma$-OH of Thr316 (2.7 Å). This interaction with the threonine gatekeeper of Lck is most likely responsible for the observed selectivity over KDR, which possesses a valine at this position. Although p38α also contains a threonine side-chain in the gatekeeper position, the most common conformation observed for this threonine in p38α structures available through the Protein Data Bank positions the $\gamma$-OH away from the ATP-binding site where it mediates a hydrogen bond between main chain atoms from strands $\beta$4 and $\beta$5.[28] This side-chain conformation positions the $\gamma$-methyl of Thr106 near the ATP-binding pocket, which would yield an unfavorable interaction with the carbonyl of **25**. However, two structures of apo p38α have been reported in which the Thr106 side chain adopts a conformation similar to that seen in the Lck structures presented here.[29] Selectivity of this series of compounds over p38α may instead result from the presence of Ile84 on strand $\beta$4 of p38α, which places a $\delta$-methyl group in close proximity to the tetracycle carbonyl oxygen (~2.5 Å; model not shown). The equivalent residue in all Src-family kinases is a valine, with the $\gamma$-methyl of this valine (301) in Lck residing 3.5 Å away from the carbonyl oxygen of **25**.

**Kinase Selectivity Profile.** To evaluate tetracyclic pyrimidine **25** in an in vivo setting, it was critical to understand the selectivity profile of this molecule. To that end, compound **25** was assayed against an extended panel of tyrosine and serine/threonine kinases (Table 4).[30] Within the protein tyrosine kinase (PTK) group, tetracycle **25** was selective (>100-fold) over representatives from the VEGFR, FGFR, InsR, Tie, and Met families, with a slight decrease in selectivity (20- to 50-fold) over members of the Tec, Syk, and Jak families. Greater selectivity was seen over kinases outside of the PTK group (CMGC and AGC), as **25** demonstrated >1000-fold selectivity over MAPK, CDK, and RSK family representatives. As expected, due to the close homology of Lck to other members of the Src family, little selectivity was observed against Src or Lyn.

**Cellular Activity.** To further characterize the cellular properties of tetracycle **25**, it was subjected to a series of functional cell assays. As shown in Table 5, compound **25** exhibited good potency in the T-cell receptor-induced IL-2 secretion assay (IL-2) and also inhibited subsequent T-cell proliferation (T-cell prolif.) in the same human T -cells. When the IL-2 secretion assay was performed using human whole blood (huWB IL-2), there was only a 3-fold shift in potency. Tetracyclic pyrimidine **25** also inhibited a human mixed lymphocyte reaction (huMLR) with a 10-fold increase in potency as compared to the other in vitro cell assays utilizing purified human cells. This shift in potency is most likely due to the longer duration of the MLR assay as compared to the IL-2 secretion and proliferation assays. This compound also displayed inhibition of a mechanism-based biochemical cell assay probing Lck-dependent TCR ζ-chain phosphorylation (TCR ζ-chain). As expected, the compound showed a 10-fold reduction in potency when IL-2 was induced in a receptor-independent fashion by stimulating with phorbol ester and calcium ionophore (PMA/iono). In addition, the compound exhibited a similar level of potency when tested in a general proliferation assay using the human T-cell line, Jurkat (JKT), suggesting the possibility of some off-target kinase activity. With this promising in vitro data, we set out to examine the in vivo properties of **25**.

**Table 4.** Kinase Selectivity Profile of Compound **25**

| kinase | $IC_{50}$[a] ($\mu$M) | kinase | $IC_{50}$[a] ($\mu$M) |
|---|---|---|---|
| Lck | 0.007 | IGFR | 2.4 |
| Src | 0.042 | FGFR | 1.6 |
| Lyn | 0.021 | KDR | 5.1 |
| Syk | 0.20 | c-Kit | 0.56 |
| ZAP-70 | 1.5 | b-Raf | 0.54 |
| Tyk2 | 1.2 | JNK2 | >40 |
| JAK3 | 0.15 | JNK3 | 7.3 |
| Itk | >20 | p38α | >10 |
| Btk | 0.41 | ERK1 | >100 |
| c-Met | >10 | CDK5 | >10 |
| Tie-2 | 0.75 | MSK1 | >100 |

[a] $IC_{50}$ values are the means of two or more separate determinations, in duplicate; standard deviations were generally within ±30% of the mean.

**Table 5.** Cellular Profile of Compound **25**

| cell assay[a] | $IC_{50}$[b] ($\mu$M) |
|---|---|
| IL-2 | 0.46 |
| T-cell prolif. | 0.53 |
| huWB IL-2 | 1.2 |
| huMLR | 0.047 |
| TCR ζ-chain | 1.6 |
| PMA/iono | 5.8 |
| JKT | 0.49 |

[a] IL-2: anti-CD3/CD28-induced T-cell IL-2 secretion assay; T-cell prolif.: anti-CD3/CD28-induced T-cell proliferation assay; huWB IL-2: anti-CD3/CD28-induced T-cell IL-2 secretion assay using human whole blood; huMLR: human mixed lymphocyte reaction; TCR ζ-chain: T-cell receptor ζ-chain phosphorylation assay; PMA/iono: anti-CD3/CD28-induced T-cell IL-2 secretion assay stimulated with phorbol myristic acid and calcium ionophore; JKT: Jurkat proliferation/survival assay. See Experimental Section for a description of each assay. [b] $IC_{50}$ values are the means of two or more separate determinations, in duplicate; standard deviations were generally within ±30% of the mean.

**Table 6.** Pharmacokinetic Parameters for Compound **25** following IV Dose in Sprague–Dawley Rats[a]

| dose[b] (mg/kg) | $AUC_{0-\infty}$ (ng h/mL) | CL (L/h/kg) | $V_{ss}$ (L/kg) | $t_{1/2}$ (h) |
|---|---|---|---|---|
| 2 | 1153 ± 137 | 1.8 ± 0.3 | 7.5 ± 1.4 | 3.12 ± 0.04 |

[a] $n = 3$ animals per study. [b] Dosed as a solution in DMSO.

**Pharmacokinetic Profile.** The pharmacokinetic properties of tetracyclic pyrimidine **25** were assessed in the rat following both intravenous (i.v.) and oral (p.o.) dosing (Tables 6 and 7, respectively). The compound displayed a moderate clearance (1.8 L/h/kg) and high volume of distribution ($V_{ss}$ = 7.5 L/kg), resulting in a half-life of 3.12 h after i.v. dosing. When dosed

**Table 7.** Pharmacokinetic Parameters for Compound **25** following Oral Dose in Sprague–Dawley Rats[a]

| dose[b] (mg/kg) | $C_{max}$ (ng/mL) | $t_{max}$ (h) | $AUC_{0-\infty}$ (ng h/mL) | bioavailability, $F$ (%) |
|---|---|---|---|---|
| 5 | 82 ± 8 | 3.0 ± 1.0 | 862 ± 34 | 17 |

[a] $n = 2$ animals per study. [b] Dosed as an aqueous suspension in 1% Tween 80 in 2% HPMC.

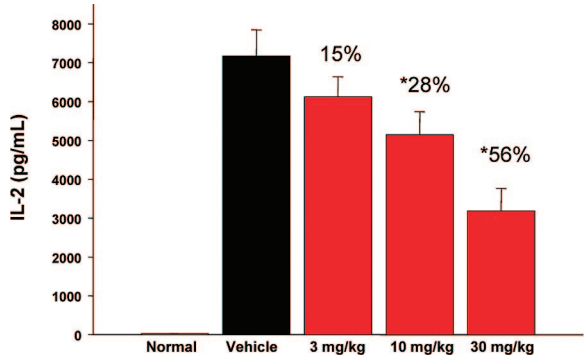


**Figure 5.** Effect of compound**25** on anti-CD3-induced IL-2 production in mice. BALB/c mice were dosed 1 h prior to challenge with compound p.o. (eight per group), as described in the Experimental Section. Mice were then challenged i.v. with antimouse CD3$\epsilon$ monoclonal antibody. A total of 90 min after the challenge, IL-2 levels in serum were determined by ELISA. Data points represent the mean IL-2 levels/group ± the standard error. $P$ values were determined vs vehicle control by Mann–Whitney U-test. *Indicates $P \leq 0.05$. From this experiment, the $ED_{50}$ of compound **25** was estimated at 26 mg/kg.

p.o. (5 mpk administered as an aqueous suspension in 1% Tween 80 in 2% HPMC), compound **25** had a $t_{max}$ of 3.0 h, with a relatively low bioavailability (17%), but was still a suitable tool for further proof of concept studies.

**Pharmacodynamic Profile.** On the basis of its PK and selectivity profile, tetracyclic pyrimidine **25** was tested in a short-term T-cell receptor dependent mouse model. A single dose of **25** was administered at 3, 10, and 30 mg/kg orally to mice and evaluated for its ability to inhibit anti-CD3-mediated IL-2 secretion in serum (Figure 5). The compound showed a dose-dependent inhibition of IL-2 production with an $ED_{50}$ estimated at 26 mg/kg.

**In Vivo Arthritis Models.** Based on its promising activity in the in vivo mouse IL-2 model, compound **25** was tested in two in vivo disease models of arthritis. In the adjuvant-induced arthritis model, arthritis was induced by injection of a suspension of *Mycobacterium tuberculosis* H37Ra in paraffin oil (0.5 mg/rat) into the base of the tail of male Lewis rats, and the disease was allowed to progress for 9 days. A once daily dose of **25** was administered orally at 10, 30, and 60 mg/kg from day 9 to day 17. Paw volume was measured daily from day 9 through day 18. The compound showed a dose-dependent inhibition of arthritis, with an $ED_{50}$ estimated at 24 mg/kg (Figure 6). Based on the measured plasma levels from the three dose groups, the exposure of **25** at the $ED_{50}$ was estimated to be 2.7 $\mu$M·h ($C_{max} \approx 0.7$ $\mu$M). In a separate study, arthritis was induced by intradermal injection of Porcine type II collagen emulsified in IFA to female Lewis rats. Disease onset occurred 10–12 days following immunization. Compound **25** was administered orally at 0.3, 1, 3, and 10 mg/kg once daily for 7 days. The anti-inflammatory effect of **25** was determined by measuring paw diameter daily for 7 days. Compound **25** showed a dose-dependent inhibition of arthritis with an $ED_{50}$ estimated at 3.2 mg/kg (Figure 7). Based on the measured plasma levels from the three dose groups, the exposure of **25** at the $ED_{50}$ was estimated to be 3.3 $\mu$M·h ($C_{max} \approx 0.5$ $\mu$M).

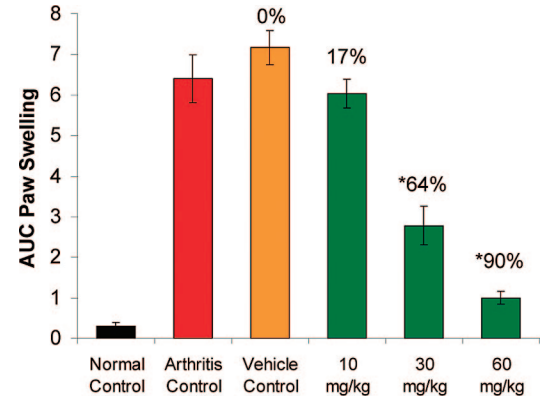


**Figure 6.** Effect of compound **25** on adjuvant-induced arthritis in the rat. Arthritis was induced by administration of *Mycobacterium tuberculosis* H37Ra suspended in paraffin oil and injected into the base of the tail (0.5 mg/rat) on day 0 to male Lewis rats (~250 g, obtained from CRL, Andover, MA). Compound **25** or vehicle was administered orally, once daily from day 9 to day 17. Paw volume was measured daily from day 9 through day 18. Values represent the mean ± standard error for $N = 8$ animals per group. *Indicates $P < 0.05$ vs vehicle control by Mann–Whitney U-test. From this experiment, the $ED_{50}$ of **25** was estimated as 24 mg/kg (AUC, 2.7 $\mu$M·h; $C_{max}$, 0.7 $\mu$M).

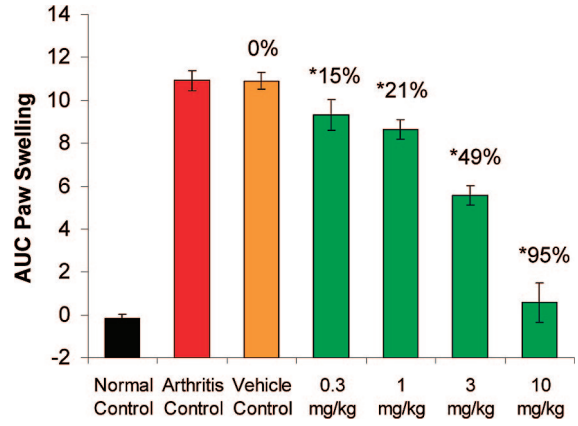


**Figure 7.** Effect of compound **25** on collagen-induced arthritis in the rat. Arthritis was induced by intradermal injection of Porcine type II collagen emulsified in IFA to female Lewis rats. Animals were assigned to a treatment group at disease onset (study day 0), which occurred 10–12 days following immunization. Compound **25** or vehicle was administered orally, once daily for 7 days. Paw diameter was measured daily from day 0 through day 7. Values represent the mean ± standard error for $N = 8$ animals per group. *Indicates $P < 0.05$ vs vehicle control by Mann–Whitney U-test. From this experiment, the $ED_{50}$ of **25** was estimated as 3.2 mg/kg (AUC, 3.3 $\mu$M·h; $C_{max}$, 0.5 $\mu$M).

## Conclusions

The novel 2-amino-6-phenylpyrimido[5′,4′:5,6]pyrimido[1,2-*a*]benzimidazol-5(6*H*)-ones have been shown to be potent and selective inhibitors of Lck. Our investigation of this series of compounds combined with structural analysis has identified the key components necessary for kinase inhibition and selectivity. Optimization efforts led to tetracyclic pyrimidine **25**, which exhibits potent and selective inhibition of Lck kinase activity. This activity translates into mechanism-based inhibition of cell-

based T-cell activation in vitro and in vivo and disease modification of T-cell mediated arthritis.

## Experimental Section

Unless otherwise noted, all materials were obtained from commercial suppliers and used without further purification. The synthesis of anilines **14a–h** has been previously reported.[13a] 4-(3-Piperidin-1-yl-propoxy)-phenylamine (**14i**) was prepared as previously reported.[31] 4-(2-(Dimethylamino)ethoxy)-3-methoxyaniline was obtained from Evotec OAI, Oxon, U.K. Anhydrous solvents were obtained from Aldrich and used directly. All reactions involving air- or moisture-sensitive reagents were performed under a nitrogen or argon atmosphere. All final compounds were purified to >95% purity, as determined by high-performance liquid chromatography (HPLC). Purity was measured using Agilent 1100 Series high performance liquid chromatography (HPLC) systems with UV detection at 254 nm (System A: Agilent Zorbax Eclipse XDB-C8 4.6 × 150 mm, 5 $\mu$m, 5 to 100% $CH_3CN$ in $H_2O$, with 0.1% TFA, for 15 min at 1.5 mL/min; System B: Zorbax SB-C8, 4.6 × 75 mm, 10 to 90% $CH_3CN$ in $H_2O$, with 0.1% formic acid, for 12 min at 1.0 mL/min). Silica gel columns were performed using either glass columns packed with silica gel (200–400 mesh, Aldrich Chemical) or prepacked silica gel cartridges (Biotage). $^1$H NMR spectra were recorded on a Bruker AV-400 (400 MHz) spectrometer or a Varian 400 MHz spectrometer at ambient temperature. All observed protons are reported as parts per million (ppm) downfield from tetramethylsilane (TMS) or other internal reference in the appropriate solvent indicated. Data are reported as follows: chemical shift, multiplicity (s = singlet, d = doublet, t = triplet, q = quartet, br = broad, m = multiplet), coupling constants, and number of protons. Low-resolution mass spectral (MS) data were determined on an Agilent 1100 Series LCMS with UV detection at 254 nm and a low resonance electrospray mode (ESI). High resolution mass spectra were obtained on a high resonance electrospray time-of-flight mass spectrometer. Combustion analysis was performed by Galbraith Laboratories, Knoxville, TN, and were within 0.4% of calculated, unless otherwise noted.

***N*-(2,6-Dimethylphenyl)-1*H*-benzo[*d*]imidazol-2-amine Hydrochloride (19a).** A mixture of 2-chlorobenzimidazole (0.500 g, 3.28 mmol) and 2,6-dimethylaniline (2.94 g, 3.00 mL, 24.2 mmol) was heated at 100 °C for 24 h. The mixture was cooled to room temperature, and the solvent was removed under reduced pressure to afford an oily residue. Trituration with ethyl acetate afforded *N*-(2,6-dimethylphenyl)-1*H*-benzo[*d*]imidazol-2-amine hydrochloride (**19a**; 0.707 g, 79%) as a dark purple solid. $^1$H NMR (400 MHz, DMSO-$d_6$) $\delta$ ppm 2.24 (s, 6 H), 7.13 – 7.56 (m, 7 H), 10.78 (s, 1 H), 12.73 (s, 2 H). MS (ESI, pos. ion) *m*/*z* 238 (M + 1).

**6-(2,6-Dimethylphenyl)-2-methylthio-benzo[4,5]imidazolo-[1,2-*a*]pyrimido[5,6-*e*]pyrimidin-5-one (21a).** A mixture of ethyl 4-chloro-2-methylthiopyrimidine-5-carboxylate (**20**; 12.5 g, 54 mmol), *N*-(2,6-dimethylphenyl)-1*H*-benzo[*d*]imidazol-2-amine hydrochloride (**19a**; 13.5 g, 49 mmol), and *N*,*N*-diisopropylethylamine (17.6 mL, 102 mmol) in toluene (30 mL) was refluxed for 3 days. The solvent was removed under reduced pressure and the residue was partitioned between dichloromethane and 2 N HCl (aq). The organic phase was washed with additional 2 N HCl (aq) and then brine. The resulting suspension was then dissolved completely by heating and concentrated to 100 mL. The resulting suspension was filtered, and the solids were washed with dichloromethane and dried to afford 6-(2,6-dimethylphenyl)-2-methylthio-benzo[4,5]imidazolo[1,2-*a*]pyrimido[5,6-*e*]pyrimidin-5-one (**21a**; 12.5 g, 60%) as a white amorphous solid. $^1$H NMR (400 MHz, $D_2O$) $\delta$ ppm 2.3 (s, 6 H), 3.0 (s, 3 H), 7.2–7.3 (m, 2 H), 7.5–7.7 (m, 3 H), 7.8 (m, 1 H), 8.75 (m, 1 H), 9.5 (s, 1 H). MS (ESI, pos. ion) *m*/*z* 388 (M + 1).

**6-(2,6-Dimethylphenyl)-2-methanesulphonyl-benzo[4,5]-imidazolo[1,2-*a*]pyrimido[5,4-*e*]pyrimidin-5-one (22a).** 6-(2,6-Dimethylphenyl)-2-methylthio-benzo[4,5]imidazolo[1,2-*a*]pyrimido[5,6-*e*]pyrimidin-5-one (**21a**; 2.00 g, 5.16 mmol) was suspended in chloroform (50 mL), and a solution of *m*-chloroperoxybenzoic acid (70%, 2.79 g, 11.3 mmol) in chloroform (50 mL, predried over anhydrous magnesium sulfate prior to addition) was added dropwise. The mixture was stirred for 15 h, dimethylsulphoxide (1.5 mL) was added, and the mixture was stirred for 1 h. Water (10 mL) was added and the organic layer was separated and washed with water, saturated aqueous sodium bicarbonate solution (twice), and brine. The solvent was removed under reduced pressure to give 6-(2,6-dimethylphenyl)-2-methanesulphonyl-benzo[4,5]imidazolo[1,2-*a*]pyrimido[5,4-*e*]pyrimidin-5-one (**22a**; 2.10 g, 97%) as a yellow solid. $^1$H NMR (400 MHz, $D_2O$) $\delta$ ppm 2.1 (s, 6 H), 3.5 (s, 3 H), 7.2–7.5 (m, 5 H), 7.6 (m, 1 H), 8.6 (m, 1 H), 9.6 (s, 1 H). MS (ESI, pos. ion) *m*/*z* 420 (M + 1).

**6-(2,6-Dimethylphenyl)-2-((4-(4-methyl-1-piperazinyl)phenyl)amino)pyrimido[5′,4′:5,6]pyrimido[1,2-*a*]benzimidazol-5(6*H*)-one (25).** A sealed tube was charged with 6-(2,6-dimethylphenyl)-2-methanesulphonyl-benzo[4,5]imidazolo[1,2-*a*]pyrimido[5,4-*e*]pyrimidin-5-one (**22a**; 3.8 g, 9.0 mmol), 4-(4-methylpiperazin-1-yl)aniline (1.8 g, 10.0 mmol), and isopropanol (75 mL). The tube was flushed with nitrogen for 2 min, fitted with a screw-cap lid, and heated at 85 °C for 15 h. The reaction mixture was cooled to room temperature and concentrated. The green residue was partitioned between dichloromethane and 1 M aqueous sodium hydroxide solution. The aqueous phase was separated and extracted with dichloromethane. The combined organic layers were dried over anhydrous magnesium sulfate, filtered, and concentrated to give a dark green oil. This material was purified via column chromatography on silica gel (eluting with 10% methanol−dichloromethane) to afford 6-(2,6-dimethylphenyl)-2-((4-(4-methyl-1-piperazinyl)phenyl)amino)pyrimido[5′,4′:5,6]pyrimido[1,2-*a*]benzimidazol-5(6*H*)-one (**25**; 2.76 g, 58%) as a yellow solid. $^1$H NMR (400 MHz, DMSO-$d_6$) $\delta$ ppm 2.05 (s, 6 H), 2.25 (s, 3 H), 2.45–2.54 (m, 4 H), 3.10–3.18 (m, 2 H), 3.18–3.26 (m, 2 H), 7.00 (d, $J$ = 8.4 Hz, 1 H), 7.08 (d, $J$ = 8.2 Hz, 1 H), 7.20–7.29 (m, 2 H), 7.30–7.43 (m, 3 H), 7.49–7.65 (m, 3 H), 8.36 (d, $J$ = 7.7 Hz, 1 H), 9.08 (s, 1 H), 10.55 (s, 1 H). MS (ESI, pos. ion) *m*/*z*: 531 (M + 1). HRMS ([M + H]$^+$) calcd, 531.26153; found, 531.26176. Anal. ($C_{31}H_{30}N_8 \cdot 1.5\ H_2O$) C, H, N.

**2-((4-((3-(Dimethylamino)propyl)oxy)phenyl)amino)-6-(2,6-dimethylphenyl)pyrimido[5′,4′:5,6]pyrimido[1,2-*a*]benzimidazol-5(6*H*)-one (28).** A sealed tube was charged with 6-(2,6-dimethylphenyl)-2-methanesulphonyl-benzo[4,5]imidazolo[1,2-*a*]pyrimido[5,4-*e*]pyrimidin-5-one (**22a**; 1.0 g, 2.4 mmol), 4-(3-(dimethylamino)propoxy)aniline (0.47 g, 2.6 mmol), and isopropanol (30 mL). Trifluoroacetic acid (0.60 g, 4.8 mmol) was added, and the tube was flushed with nitrogen for 2 min, fitted with a screw-cap lid, and heated at 85 °C for 15 h. The reaction mixture was cooled to room temperature and concentrated. The green residue was partitioned between dichloromethane (30 mL) and 1 M aq sodium hydroxide solution (10 mL). The aqueous phase was separated and extracted with dichloromethane. The combined organic layers were dried over anhydrous magnesium sulfate, filtered, and concentrated to give a yellow solid. This material was purified via column chromatography on silica gel (eluting with 5% methanol-dichloromethane) to afford 2-((4-((3-(dimethylamino)-propyl)oxy)phenyl)amino)-6-(2,6-dimethylphenyl)pyrimido[5′,4′:5,6]pyrimido[1,2-*a*]benzimidazol-5(6*H*)-one (**28**; 1.2 g, 93%) as a yellow solid. $^1$H NMR (400 MHz, DMSO-$d_6$) $\delta$ ppm 1.84–1.95 (m, 2 H), 2.06 (s, 6 H), 2.18 (s, 6 H), 2.34–2.45 (m, 2 H), 3.93–4.13 (m, 2 H), 6.96–7.03 (m, 1 H), 7.08 (d, $J$ = 6.3 Hz, 1 H), 7.25 (s, 1 H), 7.27 (s, 1 H), 7.30–7.41 (m, 1 H), 7.32–7.36 (m, 2 H), 7.54 (d, $J$ = 7.1 Hz, 1 H), 7.58–7.71 (m, 2 H), 8.32 (d, $J$ = 9.3 Hz, 1 H), 9.09 (s, 1 H), 10.60 (s, 1 H). MS (ESI, pos. ion) *m*/*z*: 534 (M + 1). HRMS ([M + H]$^+$) calcd, 534.26120; found, 534.26178. Anal. ($C_{31}H_{31}N_7O_2$) C, H, N.

The following compounds were synthesized according to the general procedure detailed above for compound **25**:

**6-(2,6-Dimethylphenyl)-2-((3-(methoxy)-4-(4-methyl-1-piperazinyl)phenyl)amino)pyrimido[5′,4′:5,6]pyrimido[1,2-*a*]benzimidazol-5(6*H*)-one (26).** $^1$H NMR (400 MHz, DMSO-$d_6$) $\delta$ ppm 2.06 (s, 6 H), 2.24 (s, 3 H), 2.44–2.56 (m, 4 H), 2.92–3.11 (m, 4 H), 3.80 (s, 3 H), 6.90–7.04 (m, 1 H), 7.14–7.24 (m, 1 H), 7.25 (s, 1 H), 7.27 (s, 1 H), 7.30–7.43 (m, 4 H), 7.55 (d, $J$ = 8.2 Hz, 1 H),

8.33–8.40 (m, 1 H), 9.11 (s, 1 H), 10.60 (s, 1 H). MS (ESI, pos. ion) *m/z*: 561 (M + 1). HRMS ([M + H]$^+$) calcd, 561.27210; found, 561.27267. Anal. ($C_{32}H_{32}N_8O_2 \cdot 2\ H_2O$) C, H, N.

**6-(2,6-Dimethylphenyl)-2-((3-(methoxy)-4-((2-(4-methyl-1-piperazinyl)ethyl)oxy)phenyl)amino)pyrimido[5′,4′:5,6]pyrimido[1,2-*a*]benzimidazol-5(6*H*)-one (29).** $^1$H NMR (400 MHz, DMSO-$d_6$) $\delta$ ppm 2.06 (s, 6 H), 2.17 (s, 3 H), 2.30–2.43 (m, 4 H), 2.48–2.59 (m, 4 H), 2.64–2.77 (m, 2 H), 3.79 (s, 3 H), 4.02–4.17 (m, 2 H), 7.01–7.20 (m, 2 H), 7.25 (s, 1 H), 7.27 (s, 1 H), 7.31–7.44 (m, 4 H), 7.55 (d, $J$ = 7.7 Hz, 1 H), 8.37 (d, $J$ = 6.7 Hz, 1 H), 9.11 (s, 1 H), 10.59 (s, 1 H). MS (ESI, pos. ion) *m/z*: 605 (M + 1). HRMS ([M + H]$^+$) calcd, 605.29831; found, 605.29925. Anal. ($C_{34}H_{36}N_8O_3 \cdot 7\ H_2O$) C. H: calcd, 6.90; found, 5.96; N: calcd, 15.33; found, 14.25.

**2-((3,5-Dimethoxy)-4-((2-(4-methyl-1-piperazinyl)ethyl)oxy)-phenyl)amino)-6-(2,6-dimethylphenyl)pyrimido[5′,4′:5,6]pyrimido[1,2-*a*]benzimidazol-5(6*H*)-one (30).** $^1$H NMR (400 MHz, DMSO-$d_6$) $\delta$ ppm 2.06 (s, 6 H), 2.17 (s, 3 H), 2.29–2.41 (m, 4 H), 2.46–2.55 (m, 4 H), 2.60–2.69 (m, 2 H), 3.80 (s, 6 H), 3.93–4.04 (m, 2 H), 6.98–7.06 (m, 1 H), 7.18–7.23 (m, 1 H), 7.26 (s, 1 H), 7.28 (s, 1 H), 7.31–7.40 (m, 3 H), 7.52–7.59 (m, 1 H), 8.42 (s, 1 H), 9.14 (s, 1 H), 10.60 (s, 1 H). MS (ESI, pos. ion) *m/z*: 635 (M + 1). HRMS ([M + H]$^+$) calcd, 635.30888; found, 635.30868. Anal. ($C_{35}H_{38}N_8O_4 \cdot 1.5\ H_2O$) C, H. N: calcd, 16.93; found:16.24.

**6-(2,6-Dimethylphenyl)-2-((3-fluoro-4-((2-(4-methyl-1-piperazinyl)ethyl)oxy)phenyl)amino)pyrimido[5′,4′:5,6]pyrimido-[1,2-*a*]benzimidazol-5(6*H*)-one (31).** $^1$H NMR (400 MHz, DMSO-$d_6$) $\delta$ ppm 2.06 (s, 6 H), 2.16 (s, 3 H), 2.29–2.38 (m, 4 H), 2.47–2.57 (m, 4 H), 2.68–2.78 (m, 2 H), 4.07–4.29 (m, 2 H), 7.23–7.49 (m, 7 H), 7.56 (d, $J$ = 8.8 Hz, 1 H), 7.67–7.87 (m, 1 H), 8.38 (d, $J$ = 9.7 Hz, 1 H), 9.14 (s, 1 H), 10.74 (s, 1 H). MS (ESI, pos. ion) *m/z*: 593 (M + 1). HRMS ([M + H]$^+$) calcd, 593.27833; found, 593.27937. Anal. ($C_{33}H_{33}FN_8O_2 \cdot 1\ CH_3OH$) C, H, N.

**6-(2,6-Dimethylphenyl)-2-((3-(methoxy)-4-((3-(4-methyl-1-piperazinyl)propyl)oxy)phenyl)amino)pyrimido[5′,4′:5,6]pyrimido[1,2-*a*]benzimidazol-5(6*H*)-one (34).** $^1$H NMR (400 MHz, DMSO-$d_6$) $\delta$ ppm 1.82–1.95 (m, 2 H), 2.06 (s, 6 H), 2.15 (s, 3 H), 2.24–2.48 (m, 10 H), 3.79 (s, 3 H), 3.94–4.11 (m, 2 H), 6.96–7.12 (m, 1 H), 7.13–7.24 (m, 1 H), 7.24–7.29 (m, 2 H), 7.30–7.44 (m, 4 H), 7.55 (d, $J$ = 7.8 Hz, 1 H), 8.36 (d, $J$ = 9.4 Hz, 1 H), 9.11 (s, 1 H), 10.58 (s, 1 H). MS (ESI, pos. ion) *m/z*: 619 (M + 1). HRMS ([M + H]$^+$) calcd, 619.31396; found, 619.31449. Anal. ($C_{35}H_{38}N_8O_3 \cdot 1.5\ H_2O$) C, H, N.

**2-((3,5-Dimethoxy)-4-((3-(4-methyl-1-piperazinyl)propyl)-oxy)phenyl)amino)-6-(2,6-dimethylphenyl)pyrimido[5′,4′:5,6]-pyrimido[1,2-*a*]benzimidazol-5(6*H*)-one (35).** $^1$H NMR (400 MHz, DMSO-$d_6$) $\delta$ ppm 1.74–1.88 (m, 2 H), 2.06 (s, 6 H), 2.25 (s, 3 H), 2.36–2.60 (m, 10 H), 3.79 (s, 6 H), 3.86–4.01 (m, 2 H), 7.01 (s, 1 H), 7.15–7.24 (m, 1 H), 7.24–7.30 (m, 2 H), 7.30–7.43 (m, 3 H), 7.56 (d, $J$ = 8.7 Hz, 1 H), 8.39 (s, 1 H), 9.14 (s, 1 H), 10.60 (s, 1 H). MS (ESI, pos. ion) *m/z*: 649 (M + 1). HRMS ([M + H]$^+$) calcd, 649.32453; found, 649.32443. Anal. ($C_{36}H_{40}N_8O_4 \cdot 2.5\ H_2O$) C, H, N: calcd, 16.15; found, 15.48.

**6-(2,6-Dichlorophenyl)-2-((4-(4-methyl-1-piperazinyl)phenyl)amino)pyrimido[5′,4′:5,6]pyrimido[1,2-*a*]benzimidazol-5(6*H*)-one (36).** $^1$H NMR (400 MHz, DMSO-$d_6$) $\delta$ ppm 2.27 (s, 3 H), 2.48–2.58 (m, 4 H), 3.15 (d, $J$ = 4.1 Hz, 2 H), 3.19–3.28 (m, 2 H), 7.00 (d, $J$ = 8.4 Hz, 1 H), 7.05–7.14 (m, 1 H), 7.29 (t, $J$ = 7.3 Hz, 1 H), 7.34–7.49 (m, 2 H), 7.52–7.64 (m, 2 H), 7.64–7.71 (m, 1 H), 7.75–7.83 (m, 2 H), 8.34 (d, $J$ = 7.8 Hz, 1 H), 9.11 (s, 1 H), 10.70 (s, 1 H). MS (ESI, pos. ion) *m/z*: 571 (M + 1). HPLC purity: 100% (system A), 99% (system B). HRMS ([M + H]$^+$) calcd, 571.15229; found, 571.15223.

**2-((4-(4-Methyl-1-piperazinyl)phenyl)amino)-6-(2,4,6-trichlorophenyl)pyrimido[5′,4′:5,6]pyrimido[1,2-*a*]benzimidazol-5(6*H*)-one (37).** $^1$H NMR (400 MHz, DMSO-$d_6$) $\delta$ ppm 2.25 (s, 3 H), 2.43–2.50 (m, 4 H), 3.09–3.18 (m, 2 H), 3.18–3.28 (m, 2 H), 7.00 (d, $J$ = 8.9 Hz, 1 H), 7.09 (d, $J$ = 8.8 Hz, 1 H), 7.23–7.48 (m, 2 H), 7.52–7.67 (m, 3 H), 8.06 (s, 2 H), 8.33 (d, $J$ = 7.6 Hz, 1 H), 9.05–9.19 (m, 1 H), 10.71 (s, 1 H). MS (ESI, pos. ion) *m/z*: 605 (M + 1). HRMS ([M + H]$^+$) calcd, 605.11332; found, 605.11312. Anal. ($C_{29}H_{23}Cl_3N_8O \cdot H_2O$) H. C: calcd, 55.83; found, 55.25; N: calcd, 17.96; found, 16.72.

**6-(4-Methylphenyl)-2-((4-(4-methyl-1-piperazinyl)phenyl)-amino)pyrimido[5′,4′:5,6]pyrimido[1,2-*a*]benzimidazol-5(6*H*)-one (38).** $^1$H NMR (400 MHz, DMSO-$d_6$) $\delta$ ppm 2.42 (s, 3 H), 2.50 (s, 3 H), 2.52–2.65 (m, 4 H), 2.80–3.08 (m, 4 H), 6.98–7.18 (m, 3 H), 7.19–7.29 (m, 1 H), 7.30–7.41 (m, 4 H), 7.46–7.69 (m, 3 H), 8.34 (d, $J$ = 7.3 Hz, 1 H), 9.04 (s, 1 H), 10.54 (s, 1 H). MS (ESI, pos. ion) *m/z*: 517 (M + 1). HPLC purity: 94% (system A), 95% (system B). HRMS ([M + H]$^+$) calcd, 517.24588; found, 517.24490.

**6-(3-Methylphenyl)-2-((4-(4-methyl-1-piperazinyl)phenyl)-amino)pyrimido[5′,4′:5,6]pyrimido[1,2-*a*]benzimidazol-5(6*H*)-one (39).** $^1$H NMR (400 MHz, DMSO-$d_6$) $\delta$ ppm 2.21–2.29 (m, 3 H), 2.40 (s, 3 H), 2.45–2.57 (m, 4 H), 3.05–3.27 (m, 4 H), 6.91–7.14 (m, 2 H), 7.19–7.39 (m, 5 H), 7.43–7.67 (m, 4 H), 8.34 (d, $J$ = 8.4 Hz, 1 H), 9.06 (s, 1 H), 10.51 (s, 1 H). MS (ESI, pos. ion) *m/z*: 517 (M + 1). HPLC purity: 96% (system A), 96% (system B). HRMS ([M + H]$^+$) calcd, 517.24588; found, 517.24633.

**6-(3-(Methoxy)phenyl)-2-((4-(4-methyl-1-piperazinyl)phenyl)amino)pyrimido-[5′,4′:5,6]pyrimido[1,2-*a*]benzimidazol-5(6*H*)-one (40).** $^1$H NMR (400 MHz, DMSO-$d_6$) $\delta$ ppm 2.25 (s, 3 H), 2.44–2.55 (m, 4 H), 3.07–3.24 (m, 4 H), 3.79 (s, 3 H), 6.88–7.13 (m, 5 H), 7.20–7.39 (m, 2 H), 7.44–7.69 (m, 4 H), 8.34 (d, $J$ = 7.5 Hz, 1 H), 9.06 (s, 1 H), 10.51 (s, 1 H). MS (ESI, pos. ion) *m/z*: 533 (M + 1). HPLC purity: 98% (system A), 99% (system B). HRMS ([M + H]$^+$) calcd, 533.24080; found, 533.24237.

**6-(5-Chloro-2-(methoxy)phenyl)-2-((4-(4-methyl-1-piperazinyl)phenyl)amino)-pyrimido[5′,4′:5,6]pyrimido[1,2-*a*]-benzimidazol-5(6*H*)-one (41).** $^1$H NMR (400 MHz, DMSO-$d_6$) $\delta$ ppm 2.25 (s, 3 H), 2.44–2.58 (m, 4 H), 3.05–3.27 (m, 4 H), 3.74 (s, 3 H), 6.93–7.15 (m, 2 H), 7.19–7.45 (m, 4 H), 7.48–7.69 (m, 4 H), 8.33 (d, $J$ = 7.9 Hz, 1 H), 9.07 (s, 1 H), 10.57 (s, 1 H). MS (ESI, pos. ion) *m/z*: 567 (M + 1). HPLC purity: 96% (system A), 94% (system B). HRMS ([M + H]$^+$) calcd, 567.20183; found, 567.20314.

**6-(4-(Butoxy)phenyl)-2-((4-(4-methyl-1-piperazinyl)phenyl)-amino)pyrimido[5′,4′:5,6]pyrimido[1,2-*a*]benzimidazol-5(6*H*)-one (42).** $^1$H NMR (400 MHz, DMSO-$d_6$) $\delta$ ppm 0.97 (t, $J$ = 7.4 Hz, 3 H), 1.40–1.58 (m, 2 H), 1.66–1.84 (m, 2 H), 2.26 (s, 3 H), 2.43–2.59 (m, 4 H), 3.03–3.27 (m, 4 H), 4.07 (t, $J$ = 6.5 Hz, 2 H), 6.92–7.14 (m, 4 H), 7.18–7.42 (m, 4 H), 7.43–7.69 (m, 3 H), 8.33 (d, $J$ = 6.8 Hz, 1 H), 9.03 (s, 1 H), 10.49 (s, 1 H). MS (ESI, pos. ion) *m/z*: 575 (M + 1). HPLC purity: 98% (system A), 100% (system B). HRMS ([M + H]$^+$) calcd, 575.28775; found, 575.28829.

The following compounds were synthesized according to the general procedure detailed above for compound **28**:

**6-(2,6-Dimethylphenyl)-2-((3,4,5-trimethoxyphenyl)amino)-pyrimido[5′,4′:5,6]pyrimido[1,2-*a*]benzimidazol-5(6*H*)-one (24).** $^1$H NMR (400 MHz, DMSO-$d_6$) $\delta$ ppm 2.06 (s, 6 H), 3.73 (s, 3 H), 3.81 (s, 6 H), 7.02 (s, 1 H), 7.21 (s, 1 H), 7.26 (s, 1 H), 7.28 (s, 1 H), 7.32–7.40 (m, 3 H), 7.56 (d, $J$ = 8.2 Hz, 1 H), 8.38–8.47 (m, 1 H), 9.14 (s, 1 H), 10.60 (s, 1 H). MS (ESI, pos. ion) *m/z*: 523 (M + 1). HRMS ([M + H]$^+$) calcd, 523.20883; found, 523.20942. Anal.($C_{29}H_{26}N_6O_4 \cdot 2.5\ H_2O$) C, N. H: calcd, 5.51; found, 4.75.

**2-((4-((2-(Dimethylamino)ethyl)oxy)phenyl)amino)-6-(2,6-dimethylphenyl)pyrimido[5′,4′:5,6]pyrimido[1,2-*a*]benzimidazol-5(6*H*)-one (27).** $^1$H NMR (400 MHz, DMSO-$d_6$) $\delta$ ppm 2.06 (s, 6 H), 2.20 – 2.30 (m, 6 H), 2.67 (s, 2 H), 3.99 – 4.20 (m, 2 H), 6.97 – 7.05 (m, 1 H), 7.10 (d, $J$ = 7.8 Hz, 1 H), 7.25 (s, 1 H), 7.27 (s, 1 H), 7.31 – 7.37 (m, 2 H), 7.36 – 7.41 (m, 1 H), 7.54 (d, $J$ = 6.8 Hz, 1 H), 7.58 – 7.74 (m, 2 H), 8.33 (d, $J$ = 8.5 Hz, 1 H), 9.10 (s, 1 H), 10.61 (s, 1 H). MS (ESI, pos. ion) *m/z*: 523 (M + 1). HRMS ([M + H]$^+$) calcd: 523.20883 found: 523.20942. Anal. ($C_{30}H_{29}N_7O_2 \cdot H_2O$) C, H, N.

**2-((3,5-Dimethoxy)-4-((2-(4-morpholinyl)ethyl)oxy)phenyl)-amino)-6-(2,6-dimethylphenyl)pyrimido[5′,4′:5,6]pyrimido-[1,2-*a*]benzimidazol-5(6*H*)-one (32).** $^1$H NMR (400 MHz, DMSO-$d_6$) $\delta$ ppm 2.06 (s, 6 H), 2.46–2.52 (m, 4 H), 2.62–2.70 (m, 2 H), 3.55–3.62 (m, 4 H), 3.80 (s, 6 H), 3.95–4.06 (m, 2 H), 6.98–7.06 (m, 1 H), 7.17–7.24 (m, 1 H), 7.26 (s, 1 H), 7.28 (s, 1 H), 7.32–7.40 (m, 3 H), 7.56 (d, $J$ = 8.4 Hz, 1 H), 8.37–8.46 (m, 1 H), 9.14 (s,

1 H), 10.61 (s, 1 H). MS (ESI, pos. ion) *m/z*: 622 (M + 1). HRMS ($[M + H]^+$) calcd, 622.27724; found, 622.27962. Anal. ($C_{34}H_{35}N_7O_5 \cdot 0.5\ H_2O$) C, H, N.

**6-(2,6-Dimethylphenyl)-2-((4-((3-(1-piperidinyl)propyl)oxy)-phenyl)amino)pyrimido[5′,4′:5,6]pyrimido[1,2-*a*]benzimidazol-5(6*H*)-one (33).** $^1$H NMR (400 MHz, DMSO-$d_6$) $\delta$ ppm 1.33–1.43 (m, 2 H), 1.43–1.55 (m, 4 H), 1.83–1.97 (m, 2 H), 2.06 (s, 6 H), 2.26–2.47 (m, 6 H), 3.97–4.14 (m, 2 H), 6.95–7.03 (m, 1 H), 7.08 (d, $J$ = 7.4 Hz, 1 H), 7.23–7.29 (m, 2 H), 7.30–7.43 (m, 3 H), 7.54 (d, $J$ = 7.5 Hz, 1 H), 7.58–7.71 (m, 2 H), 8.28–8.39 (m, 1 H), 9.09 (s, 1 H), 10.60 (s, 1 H). MS (ESI, pos. ion) *m/z*: 574 (M + 1). HRMS ($[M + H]^+$) calcd, 574.29250; found, 574.29376. Anal. ($C_{34}H_{35}N_7O_2 \cdot H_2O$) C, H. N: calcd, 16.57; found, 15.83.

**Lck Kinase Assay.** The Lck HTRF kinase assay involved ATP-dependent phosphorylation of a biotinylated substrate peptide of gastrin in the presence or absence of inhibitor compound. The final concentration of gastrin was 1.2 $\mu$M. The final concentration of ATP was 0.5 $\mu$M ($K_m$ app = 0.6 ± 0.1 $\mu$M) and the final concentration of Lck (a GST-kinase domain fusion (AA 225–509)) was 250 pM. Buffer conditions were as follows: 50 mM HEPES, pH = 7.5, 50 mM NaCl, 20 mM MgCl, 5 mM MnCl, 2 mM DTT, 0.05% BSA. The assay was quenched and stopped with 160 $\mu$L of detection reagent. Detection reagents were as follows: buffer was made of 50 mM Tris, pH = 7.5, 100 mM NaCl, 3 mM EDTA, 0.05% BSA, 0.1% Tween20. Prior to reading, *Streptavidin allophycocyanin* (SA-APC) was added at a final concentration in the assay of 0.0004 mg/mL, along with europilated antiphosphotyrosine Ab (Eu-anti-PY) at a final concentration of 0.025 nM. The assay plate was read in a Discovery fluorescence plate reader with excitation at 320 nm and emission at 615 and 655 nm.

Assays for other kinases were done in a similar way as described above, varying the concentrations of enzyme, peptide substrate, and ATP added to the reaction, depending on the specific activity of the kinase and measured $K_m$'s for the substrates.

**Human Mixed Lymphocyte Reaction (huMLR).** This assay tests the potency of T-cell activation inhibitors in an in vitro model of allogeneic T-cell stimulation. Human peripheral blood lymphocytes (hPBL; $2 \times 10^5$/well) were incubated with mitomycin C-treated B lymphoblastoid cells (JY cell line (ATCC, Rockville, MD); $1 \times 10^5$/well) as allogeneic stimulators in the presence or absence of dilutions of potential inhibitor compound in 96-well round-bottom tissue culture plates. These cultures were incubated at 37 °C in 5% $CO_2$ for 6 days total. The proliferative response of the hPBL was measured by $^3$H-thymidine incorporation overnight between days 5 and 6 after initiation of culture. Cells were harvested onto glass fiber filters and $^3$H-thymidine incorporation into DNA was analyzed by liquid scintillation counter.

**Jurkat Proliferation/Survival Assay.** This assay tests the general antiproliferative/cytotoxic effect of compounds on the Jurkat human T-cell line (ATCC, Rockville, MD). Jurkat cells ($1 \times 10^5$/well) were plated in 96-well flat-bottom tissue culture plates with or without compound dilutions and cultured for 72 h at 37 °C in 5% $CO_2$. Viable cell number was determined during the last 4 h of culture by adding 10 $\mu$L/well WST-8 dye (Alexis; San Diego, CA). WST-8 dye conversion relied on active mitochondrial electron transport for reduction of the tetrazolium dye. The dye conversion was read by OD at 450–600 nM.

**Anti-CD3/CD28-Induced T-Cell IL-2 Secretion and Proliferation Assay.** This assay tests the potency of T-cell receptor (TCR; CD3) and CD28 signaling pathway inhibitors in human T-cells. T-cells were purified from human peripheral blood lymphocytes (hPBL) and preincubated with or without compound prior to stimulation with a combination of an anti-CD3 and an anti-CD28 antibody in 96-well tissue culture plates ($1 \times 10^5$T cells/well). Cells were cultured for ~20 h at 37 °C in 5% $CO_2$, then secreted IL-2 in the supernatants was quantified by cytokine ELISA (Pierce/Endogen, St. Louis, MO). The cells remaining in the wells were then pulsed with $^3$H-thymidine overnight to assess the T-cell proliferative response. Cells were harvested onto glass fiber filters and $^3$H-thymidine incorporation into DNA was analyzed by liquid scintillation counter. For comparison purposes, phorbol myristic acid (PMA) and calcium ionophore were used in combination to induce IL-2 secretion from purified T-cells. Potential inhibitor compounds were tested for inhibition of this response, as described above for anti-CD3 and anti-CD28 antibodies. Human whole-blood anti-CD3/anti-CD28-induced IL-2 secretion assays were run in a similar fashion as described above using whole blood from normal volunteers diluted 50% in tissue culture medium prior to stimulation.

**TCR ζ-Chain Phosphorylation Assay.** Jurkat cells ($1.25 \times 10^6$/well) were seeded in a 96-well plate (round-bottom) in 150 $\mu$L of RPMI + 10% FCS and then preincubated with 50 $\mu$L compound or without compound (50 $\mu$L medium) at 37 °C for 30 min. For anti-CD3 stimulation, cells were cooled on ice for 15 min and then incubated with 10 $\mu$L of anti-CD3 mAb (UCHT-1) at a final concentration of 1.2 $\mu$g/mL for 30 min. A total of 20 $\mu$L of GAM-$IgG_1$ was added to cells at 30 $\mu$g/mL final and incubated for 20 min on ice. Cells were transferred to a 37 °C water bath and stimulated for 1 min. Cells were spun at speed 1000 rpm in the centrifuge for 5 min. Supernatant was aspirated and cells were lysed in 30 $\mu$L of cold lysis buffer (1% Triton X-100 in NaCl/HEPES) with phosphatase/protease inhibitors for 30 min on ice. Lysates were spun at 3000 rpm in the centrifuge for 5 min to remove nuclei before 25 $\mu$L of supernatant was transferred to new tubes for the Igen ζ-chain phosphorylation detection assay.

A master mix was made containing (vol. per sample tube) 21 $\mu$L of Igen dilution buffer (PBS, 1% BSA, 0.1% tween-20; Igen/BioVeris; Gaithersburg, MD), 4 $\mu$L of the capture antibody, antihuman CD247 mAb, clone G3 (BD Coulter, San Diego, CA), coupled with Dynabeads M-280, 200 $\mu$L of the detection antibody, ruthenylated p-CD3-ζ (415.9A; Santa Cruz Biotech., Santa Cruz, CA) at 1 to 16000 dilution in Igen dilution buffer. A total of 25 $\mu$L per sample lysate was transferred from the lysate plate to a tube including the negative and positive controls. Sample tubes were shaken at room temperature overnight. Tubes then were placed in a carousel of Igen tube analyzer and analyzed. The signal-to-noise ratio was generally around 15–20.

The procedure of coupling the capture antibody, antihuman CD247 mAb, clone G3 to Dynabeads M-280 was based on the protocol provided by Dynal Biotech. The procedure of p-CD3-ζ ruthenylation is based on the protocol provided by Bio Veris.

**Pharmacokinetic Studies.** Sprague–Dawley rats were administered a solution of compound in DMSO at the indicated doses i.v. For oral dosing, a suspension of the compound in 2% hydroxypropyl methylcellulose with 1% Tween-80 was administered. Samples were taken at the indicated times and analyzed for parent compound by LC-MS.

**Anti-CD3-Induced IL-2 Production in Mice.** Twelve week old (20 g) BALB/c mice were dosed 1 h prior to challenge with compound p.o. (eight per group) at the indicated doses in 2% hydroxypropyl methylcellulose with 1% Tween-80. Mice were then challenged i.v. with antimouse CD3ϵ monoclonal antibody (145.2C11, BD PharMingen, San Diego, CA; 3 $\mu$g/mouse) diluted in PBS. A total of 90 min after anti-CD3 challenge, blood was collected via cardiac puncture. IL-2 levels were measured in serum by ELISA (BioSource, Camarillo, CA). Data points represent the mean IL-2 levels/group ± the standard error. $P$ values were determined versus vehicle control by Mann–Whitney U-test.

**Adjuvant-Induced Arthritis in Rats.** Arthritis was induced on day 0 by injection of *Mycobacterium tuberculosis* H37Ra suspended in paraffin oil (0.5 mg/rat) into the base of the tail of male Lewis rats (~250 g, obtained from CRL, Andover, MA). The compound or vehicle (2% hydroxypropyl methylcellulose with 1% Tween-80) was administered orally, once daily from day 9 to day 17. Paw volume was measured daily from day 9 through day 18. Values represent the mean ± standard error for $N = 8$ animals per group. $^*P < 0.05$ versus vehicle control by Mann–Whitney U-test.

**Collagen-Induced Arthritis in Rats.** Arthritis was induced by intradermal injection of Porcine type II collagen emulsified in IFA to female Lewis rats. Animals were assigned to treatment group at disease onset (study day 0), which occurred 10–12 days following immunization. The compound or vehicle (2% hydroxypropyl methylcellulose with 1% Tween-80) was administered orally, once

daily for 7 days. Paw diameter was measured daily from day 0 through day 7. Values represent the mean ± standard error for $N = 8$ animals per group. $^*P < 0.05$ versus vehicle control by Mann–Whitney U-test.

**SIF Solubility Assay.** The solubility media was fasted state simulated intestinal fluid (SIF), pH 6.8, containing 5 mM sodium taurochol, 1.5 mM lecithin, 2.9 mM $KH_2PO_4$, and 0.22 M KCl. The Symyx solubility system (Santa Clara, CA) consisted of a liquid handling robot and an Agilent 1100 HPLC. An experiment template was created for solubility measurements of 24 compounds on a 96-well plate. Samples were prepared assuming a screening criterion of 200 μg/mL solubility. A stock solution was first prepared for each of the 24 compounds on a 24-well plate. A mixed solution of 50/50 $CH_3OH$/DME (v/v) was used as the stock solvent. The weight of the solid sample (i.e., 1 mg, to the nearest 0.01 mg) was directly imported, and the appropriate volume of the stock solvent was calculated and dispensed into the 4 mL vial for each compound by the liquid handling robot to obtain a stock concentration of 500 μg/mL. From each of the 24 compound stock solutions, volumes of 200, 250, 250, and 250 μL were robotically transferred to an array of four 1 mL glass vials on a 96-well plate: one vial for the calibration standard and the other three vials for solubility samples. After evaporation of the stock solvent using a centrifugal evaporator, 500 μL of the solubility media was added to the corresponding sample vials on the 96-well plate for each compound to give a calculated concentration of 250 μg/mL. A stir bar was added to each vial using a 96-well stir bar dispenser, and the vials were sealed with a 96-well cap mat. The samples were equilibrated by stirring at 100 rpm for 24 h and subsequently left standing unstirred for an additional 24–48 h at room temperature. After equilibration, 500 μL of 50/50 $CH_3OH$/DME was added to the corresponding standard vials on the same plate for each compound to give a calibration concentration of 200 μg/mL. Immediately before solubility measurement by HPLC, the sealed 96-well plate was centrifuged at 1650 rpm for 10 min using a plate centrifuge to allow separation of the compound supernatant from undissolved solid. The solubility samples and the calibration standards in 1 mL vials on a 96-well plate were injected directly onto the HPLC column after centrifuging. A fast gradient method was developed for HPLC throughput, starting with 100% water, containing 0.04% trifluoroacetic acid (TFA) and holding for 0.1 min, then ramping to 100% acetonitrile containing 0.04% TFA in 0.1 min and holding for 1.0 min. A Phenomenex Synergi Hydro-RP C-18 column (10 mm × 2.0 mm, 2 μm) was chosen for retention and resolution of both polar and nonpolar compounds. The injection volume was 2 μL, with a detection wavelength of 220 nm. For each compound, its solubility was quantified through individual standard peak area calibration at a concentration equal to the solubility screening criterion (i.e., 200 μg/mL).

**Acknowledgment.** We thank our colleagues Alan Cheng for the model of compound **3** in Lck; Matthew Plant for the p38α kinase assay data; Isaac Marx for the resynthesis of **1** and **19a**; and Maggie Reed for the SIF solubility assay.

**Supporting Information Available:** Elemental analysis and HPLC purity data for the compounds synthesized and data collection and refinement statistics for the X-ray structures of compounds **1** and **25** bound to Lck. This material is available free of charge via the Internet at http://pubs.acs.org.

## References

(1) Kane, L. P.; Lin, J.; Weiss, A. Signal transduction by the TCR for antigen. *Curr. Opin. Immunol.* **2000**, *12*, 242–249.
(2) Bolen, J. B.; Brugge, J. S. Leukocyte protein tyrosine kinases: Potential targets for drug discovery. *Annu. Rev. Immunol.* **1997**, *15*, 371–404.
(3) Lowell, C. A.; Soriano, P. Knockouts of Src-family kinases: Stiff bones, wimpy T cells, and bad memories. *Genes Dev.* **1996**, *10*, 1845–1857.
(4) Marth, J. D.; Lewis, D. B.; Cooke, M. P.; Mellins, E. D.; Gearn, M. E.; Samelson, L. E.; Wilson, C. B.; Miller, A. D.; Perlmutter, R. M. Lymphocyte activation provokes modification of a lymphocyte specific protein tyrosine kinase (p56lck). *J. Immunol.* **1989**, *142*, 2430–2437.
(5) Groves, T.; Smiley, P.; Cooke, M. P.; Forbush, K.; Perlmutter, R. M.; Guidos, C. J. Fyn can partially substitute for Lck in T lymphocyte development. *Immunity* **1996**, *5*, 417–428.
(6) Palacios, E. H.; Weiss, A. Function of the Src-family kinases, Lck and Fyn, in T-cell development and activation. *Oncogene* **2004**, *23*, 7990–8000.
(7) Molina, T. J.; Kishihara, K.; Siderovskid, D. P.; van Ewijk, W.; Narendran, A.; Timms, E.; Wakeham, A.; Paige, C. J.; Hartmann, K.-U.; Veillette, A.; Davidson, D.; Mak, T. W. Profound block in thymocyte development in mice lacking p56lck. *Nature* **1992**, *357*, 161–164.
(8) Levin, S. D.; Anderson, S. J.; Forbush, K. A.; Perlmutter, R. M. A dominant-negative transgene defines a role for p56lck in thymopoiesis. *EMBO J.* **1993**, *12*, 1671–1680.
(9) Seddon, B.; Zamoyska, R. TCR signals mediated by Src family kinases are essential for the survival of naïve T cells. *J. Immunol.* **2002**, *169*, 2997–3005.
(10) Straus, D. B.; Weiss, A. Genetic evidence for the involvement of the lck tyrosine kinase in signal transduction through the T cell antigen receptor. *Cell* **1992**, *70*, 585–593.
(11) Goldman, F. D.; Ballas, Z. K.; Schutte, B. C.; Kemp, J.; Hollenback, C.; Noraz, N.; Taylor, N. Defective expression of p56lck in an infant with severe combined immunodeficiency. *J. Clin. Invest.* **1998**, *102*, 421–429.
(12) Hubert, P.; Bergeron, F.; Ferreirea, V.; Seligmann, M.; Oksenhendler, E.; Debre, P.; Autran, B. Defective p56lck activity in T cells from an adult patient with idiopathic $CD4^+$ lymphocytopenia. *Int. Immunol.* **2000**, *12*, 449–457.
(13) (a) Martin, M. W.; Newcomb, J.; Nunes, J. J.; McGowan, D. C.; Armistead, D. M.; Boucher, C.; Buchanan, J. L.; Buckner, W.; Chai, L.; Elbaum, D.; Epstein, L. F.; Faust, T.; Flynn, S.; Gallant, P.; Gore, A.; Gu, Y.; Hsieh, F.; Huang, X.; Lee, J. H.; Metz, D.; Middleton, S.; Mohn, D.; Morgenstern, K.; Morrison, M. J.; Novak, P. M.; Oliveira-dos-Santos, A.; Powers, D.; Rose, P.; Schneider, S.; Sell, S.; Tudor, Y.; Turci, S. M.; Welcher, A. A.; White, R. D.; Zack, D.; Zhao, H.; Zhu, L.; Zhu, X.; Ghiron, C.; Amouzegh, P.; Ermann, M.; Jenkins, J.; Johnston, D.; Napier, S.; Power, E. Novel 2-aminopyrimidine carbamates as potent and orally active inhibitors of Lck: Synthesis, SAR, and in vivo anti-inflammatory activity. *J. Med. Chem.* **2006**, *49*, 4981–4991. (b) DiMauro, E. F.; Newcomb, J.; Nunes, J. J.; Bemis, J. E.; Boucher, C.; Buchanan, J. L.; Buckner, W. H.; Cee, V. J.; Chai, L.; Deak, H. L.; Epstein, L. F.; Faust, T.; Gallant, P.; Geuns-Meyer, S. D.; Gore, A.; Gu, Y.; Henkle, B.; Hodous, B. L.; Hsieh, F.; Huang, X.; Kim, J. L.; Lee, J. H.; Martin, M. W.; Masse, C. E.; McGowan, D. C.; Metz, D.; Mohn, D.; Morgenstern, K. A.; Oliveira-dos-Santos, A.; Patel, V. F.; Powers, D.; Rose, P. E.; Schneider, S.; Tomlinson, S. A.; Tudor, Y.-Y.; Turci, S. M.; Welcher, A. A.; White, R. D.; Zhao, H.; Zhu, L.; Zhu, X. Discovery of aminoquinazolines as potent, orally bioavailable inhibitors of Lck: Synthesis, SAR, and in vivo anti-inflammatory activity. *J. Med. Chem.* **2006**, *49*, 5671–5686. (c) Martin, M. W.; Newcomb, J.; Nunes, J. J.; Bemis, J. E.; McGowan, D. C.; White, R. D.; Buchanan, J. L.; DiMauro, E. F.; Boucher, C.; Faust, T.; Hsieh, F.; Huang, X.; Lee, J. H.; Schneider, S.; Turci, S. M.; Zhu, X. Discovery of novel 2,3-diarylfuro[2,3-*b*]pyridine-4-amines as potent and selective inhibitors of Lck: Synthesis, SAR, and pharmacokinetic properties. *Bioorg. Med. Chem. Lett.* **2007**, *17*, 2299–2304. (d) DiMauro, E. F.; Newcomb, J.; Nunes, J. J.; Bemis, J. E.; Boucher, C.; Buchanan, J. L.; Buckner, W. H.; Chang, A.; Faust, T.; Hsieh, F.; Huang, X.; Lee, J. H.; Marshall, T. L.; Martin, M. W.; McGowan, D. C.; Schneider, S.; Turci, S. M.; White, R. D.; Zhu, X. Discovery of 4-amino-5,6-biaryl-furo[2,3-*d*]pyrimidines as inhibitors of Lck: Development of an expedient and divergent synthetic route and preliminary SAR. *Bioorg. Med. Chem. Lett.* **2007**, *17*, 2305–2309. (e) Deak, H. L.; Newcomb, J. R.; Nunes, J. J.; Boucher, C.; Cheng, A. C.; DiMauro, E. F.; Epstein, L. F.; Gallant, P.; Hodous, B. L.; Huang, X.; Lee, J. H.; Patel, V. F.; Schneider, S; Turci, S. M.; Zhu, X. *N*-(3-(Phenylcarbamoyl)arylpyrimidine)-5-carboxamides as potent and selective inhibitors of Lck: Structure, synthesis, and SAR. *Bioorg. Med. Chem. Lett.* **2008**, *18*, 1172–1176. (f) DiMauro, E. F.; Newcomb, J.; Nunes, J. J.; Bemis, J. E.; Boucher, C.; Chai, L.; Chaffee, S. C.; Deak, H. L.; Epstein, L. F.; Faust, T.; Gallant, P.; Gore, A.; Gu, Y.; Henkle, B.; Hsieh, F.; Huang, X.; Kim, J. L.; Lee, J. H.; Martin, M. W.; McGowan, D. C.; Metz, D.; Mohn, D.; Morgenstern, K. A.; Oliveira-dos-Santos, A.; Patel, V. F.; Powers, D.; Rose, P. E.; Schneider, S.; Tomlinson, S. A.; Tudor, Y.-Y.; Turci, S. M.; Welcher, A. A.; Zhao, H.; Zhu, L.; Zhu, X. Structure-guided design of aminopyrimidine amides as potent, selective inhibitors of Lck: Synthesis, SAR, and inhibition of in vivo T-cell activation. *J. Med. Chem.* **2008**, *51*, 1681–1694.
(14) Hanke, J. H.; Gardner, J. P.; Dow, R. L.; Changelian, P. S.; Brissette, W. H.; Weringer, E. J.; Pollok, B. A.; Connelly, P. A. Discovery of a novel, potent, and Src-family-selective tyrosine kinase inhibitor. *J. Biol. Chem.* **1996**, *271*, 695–701.

(15) Trevillyan, J. M.; Chiou, X. G.; Ballaron, S. J.; Tang, Q. M.; Buko, A.; Sheets, M. P.; Smith, M. L.; Putnam, B.; Wiedeman, P.; Tu, N.; Madar, D.; Smith, H. T.; Gubbins, E. J.; Warrior, U. P.; Chen, Y.-W.; Mollison, K. W.; Faltynek, C. R.; Djuric, S. W. Inhibition of p56lck tyrosine kinase by isothiazoles. *Arch. Biochem. Biophys.* **1999**, *364*, 19–29.

(16) (a) Snow, R. J.; Cardozo, M. G.; Morwick, T. M.; Busacca, C. A.; Dong, Y.; Eckner, R. J.; Jacober, S.; Jakes, S.; Kapadia, S.; Lukas, S.; Panzenbeck, M.; Peet, G. W.; Peterson, J. D.; Prokopowicz, A. S.; Sellati, R.; Tolbert, R. M.; Tschantz, M. A.; Moss, N. Discovery of 2-phenylamino-imidazo[4,5-*h*]isoquinolin-9-ones: A new class of inhibitors of Lck kinase. *J. Med. Chem.* **2002**, *45*, 3394–3405. (b) Goldberg, D. R.; Butz, T.; Cardozo, M. G.; Eckner, R. J.; Hammach, A.; Huang, J.; Jakes, S.; Kapadia, S.; Kashem, M.; Lukas, S.; Morwick, T. M.; Panzenbeck, M.; Patel, U.; Pav, S.; Peet, G. W.; Peterson, J. D.; Prokopowicz, A. S.; Snow, R. J.; Sellati, R.; Takahashi, H.; Tan, J.; Tschantz, M. A.; Wang, X.-J.; Wang, Y.; Wolak, J.; Xiong, P.; Moss, N. Optimization of 2-phenylaminoimidazo[4,5-*h*]isoquinolin-9-ones: Orally active inhibitors of lck kinase. *J. Med. Chem.* **2003**, *46*, 1337–1349.

(17) (a) Chen, P.; Norris, D.; Iwanowicz, E. J.; Spergel, S. H.; Lin, J.; Gu, H. H.; Shen, Z.; Wityak, J.; Lin, T.-A.; Pang, S.; de Fex, H.; Pitt, S.; Shen, D. R.; Doweyko, A. M.; Bassolino, D. A.; Roberge, J. Y.; Poss, M. A.; Chen, B.-C.; Schieven, G. L.; Barrish, J. C. Discovery and initial SAR of imidazoquinoxalines as inhibitors of the Src-family kinase p56Lck. *Bioorg. Med. Chem. Lett.* **2002**, *12*, 1361–1364. (b) Chen, P.; Iwanowicz, E. J.; Norris, D.; Gu, H. H.; Lin, J.; Moquin, R. V.; Das, J.; Wityak, J.; Spergel, S. H.; de Fex, H.; Pang, S.; Pitt, S.; Shen, D. R.; Schieven, G. L.; Barrish, J. C. Synthesis and SAR of novel imidazoquinoxaline-based Lck inhibitors: Improvement of cell potency. *Bioorg. Med. Chem. Lett.* **2002**, *12*, 3153–3156. (c) Das, J.; Lin, J.; Moquin, R. V.; Shen, Z.; Spergel, S. H.; Wityak, J.; Doweyko, A. M.; DeFex, H. F.; Fang, Q.; Pang, S.; Pitt, S.; Shen, D. R.; Schieven, G. L.; Barrish, J. C. Molecular design, synthesis, and structure−activity relationships leading to the potent and selective P56lck inhibitor BMS-243117. *Bioorg. Med. Chem. Lett.* **2003**, *13*, 2145–2149. (d) Das, J.; Moquin, R. V.; Lin, J.; Liu, C.; Doweyko, A. M.; DeFex, H. F.; Fang, Q.; Pang, S.; Pitt, S.; Shen, D. R.; Schieven, G. L.; Barrish, J. C.; Wityak, J. Discovery of 2-amino-heteroaryl-benzothiazole-6-anilides as potent p56lck inhibitors. *Bioorg. Med. Chem. Lett.* **2003**, *13*, 2587–2590. (e) Chen, P.; Norris, D.; Das, J.; Spergel, S. H.; Wityak, J.; Leith, L.; Zhao, R.; Chen, B.-C.; Pitt, S.; Pang, S.; Shen, D. R.; Zhang, R.; De Fex, H. F.; Doweyko, A. M.; McIntyre, K. W.; Shuster, D. J.; Behnia, K.; Schieven, G. L.; Barrish, J. C. Discovery of novel 2-(aminoheteroaryl)-thiazole-5-carboxamides as potent and orally active Src-family kinase p56lck inhibitors. *Bioorg. Med. Chem. Lett.* **2004**, *14*, 6061–6066. (f) Chen, P.; Doweyko, A. M.; Norris, D.; Gu, H. H.; Spergel, S. H.; Das, J.; Moquin, R. V.; Lin, J.; Wityak, J.; Iwanowicz, E. J.; McIntyre, K. W.; Shuster, D. J.; Behnia, K.; Chong, S.; de Fex, H.; Pang, S.; Pitt, S.; Shen, D. R.; Thrall, S.; Stanley, P.; Kocy, O. R.; Witmer, M. R.; Kanner, S. B.; Schieven, G. L.; Barrish, J. C. Imidazoquinoxaline Src-family kinase p56Lck inhibitors: SAR, QSAR, and the discovery of (*S*)-*N*-(2-chloro-6-methylphenyl)-2-(3-methyl-1-piperazinyl)imidazo- [1,5-*a*]pyrido[3,2-*e*]pyrazin-6-amine (BMS-279700) as a potent and orally active inhibitor with excellent in vivo anti-inflammatory activity. *J. Med. Chem.* **2004**, *47*, 4517–4529.

(18) (a) Arnold, L. D.; Calderwood, D. J.; Dixon, R. W.; Johnston, D. N.; Kamens, J. S.; Munschauer, R.; Rafferty, P.; Ratnofsky, S. E. Pyrrolo[2,3-*d*]pyrimidines containing an extended 5-substituent as potent and selective inhibitors of lck II. *Bioorg. Med. Chem. Lett.* **2000**, *10*, 2167–2170. (b) Burchat, A. F.; Calderwood, D. J.; Friedman, M. M.; Hirst, G. C.; Li, B.; Rafferty, P.; Ritter, K.; Skinner, B. S. Pyrazolo[3,4-*d*]pyrimidines containing an extended 3-substituent as potent inhibitors of Lck-a selectivity insight. *Bioorg. Med. Chem. Lett.* **2002**, *12*, 1687–1690. (c) Borhani, D. W.; Calderwood, D. J.; Friedman, M. M.; Hirst, G. C.; Li, B.; Leung, K. W.; McRae, B.; Ratnofsky, S.; Ritter, K.; Waegell, W. A-420983: A potent, orally active inhibitor of Lck with efficacy in a model of transplant rejection. *Bioorg. Med. Chem. Lett.* **2004**, *14*, 2613–2616. (d) Burchat, A.; Borhani, D. W.; Claderwood, D. J.; Hirst, G. C.; Li, B.; Stachlewitz, R. F. Discovery of A-770041, a src-family selective orally active Lck inhibitor that prevents organ allograft rejection. *Bioorg. Med. Chem. Lett.* **2006**, *16*, 118–122. (e) Abbott, L.; Betschmann, P.; Burchat, A.; Calderwood, D. J.; Davis, H.; Hrnciar, P.; Hirst, G. C.; Li, B.; Morytko, M.; Mullen, K.; Yang, B. Discovery of thienopyridines as Src-family selective Lck inhibitors. *Bioorg. Med. Chem. Lett.* **2007**, *17*, 1167–1171.

(19) (a) Maier, J. A.; Brugel, T. A.; Sabat, M.; Golebiowski, A.; Laufersweiler, M. J.; VanRens, J. C.; Hopkins, C. R.; De, B.; Hsieh, L. C.; Brown, K. K.; Easwaran, V.; Janusz, M. J. Development of *N*-4,6-pyrimidine-*N*-alkyl-*N*′-phenyl ureas as orally active inhibitors of lymphocyte specific tyrosine kinase. *Bioorg. Med. Chem. Lett.* **2006**, *16*, 3646–3650. (b) Sabat, M.; VanRens, J. C.; Brugel, T. A.; Maier, J.; Laufersweiler, M. J.; Golebiowski, A.; De, B.; Easwaran, V.; Hsieh, L. C.; Rosegan, J.; Berberich, S.; Suchanek, E.; Janusz, M. J. The development of novel 1,2-dihydro-pyrido[4,5-*c*]pyridazine based inhibitors of lymphocyte specific kinase (Lck). *Bioorg. Med. Chem. Lett.* **2006**, *16*, 4257–4261. (c) Sabat, M.; VanRens, J. C.; Laufersweiler, M. J.; Brugel, T. A.; Maier, J.; Golebiowski, A.; De, B.; Easwaran, V.; Hsieh, L. C.; Walter, R. L.; Mekel, M. J.; Evdokimov, A.; Janusz, M. J. The development of 2-benzimidazole substituted pyrimidine based inhibitors of lymphocyte specific kinase (Lck). *Bioorg. Med. Chem. Lett.* **2006**, *16*, 5973–5977.

(20) (a) Waegell, W.; Babineau, M.; Hart, M.; Dixon, K.; McRae, B.; Wallace, C.; Leach, M.; Ratnofsky, S.; Belanger, A.; Hirst, G.; Rossini, A.; Appel, M.; Mordes, J.; Greiner, D.; Banerjee, S. A420983, a novel, small molecule inhibitor of Lck prevents allograft rejection. *Transplant. Proc.* **2002**, *34*, 1411–1417. (b) McRae, B. L.; Wallace, C.; Dixon, K. F.; Roux, A.; Mohan, S.; Jia, Y.; Presky, D. H.; Tracey, D. E.; Hirst, G. C. Suppression of CD4+ T cell activation by a novel inhibitor of Src family kinases. *Int. Immunopharmacol.* **2005**, *5*, 667–677.

(21) This observation is consistent with results we have obtained from co-crystal structures of other protein−ligand systems. For a discussion of CH-O hydrogen bonds in protein−ligand complexes, see Pierce, A. C.; Sandretto, K. L.; Bemis, G. W. Kinase inhibitors and the case for CH···O hydrogen bonds in protein−ligand binding. *Proteins: Struct., Funct., Genet.* **2002**, *49*, 567–576.

(22) The model of **3** and Lck was generated using MOE (Chemical Computing Group, Montreal, version 2006.08) based on the co-crystal structure of **1** and Lck.

(23) Because p38α also has threonine as its gatekeeper residue, we did not believe this would be an effective measure toward gaining selectivity over p38α.

(24) For the synthesis of compounds containing an aniline substituted with *N*-methylpiperazine (such as **25**), it was necessary to run the reaction without acid to avoid the formation of unwanted side products.

(25) (a) Lee, M. R.; Dominguez, C. MAP kinase p38 inhibitors: Clinical results and an intimate look at their interactions with p38α protein. *Curr. Med. Chem.* **2005**, *12*, 2979–2994. (b) Goldstein, D. M.; Gabriel, T. Pathway to the clinic: Inhibition of p38 MAP kinase. A review of ten chemotypes selected for development. *Curr. Top. Med. Chem.* **2005**, *5*, 1017–1029. (c) Hynes, J., Jr.; Leftheris, K. Small molecule p38 inhibitors: Novel structural features and advances from 2002–2005. *Curr. Top. Med. Chem.* **2005**, *5*, 967–985.

(26) (a) Ferrara, N.; Gerber, H.; LeCouter, J. The biology of VEGF and its receptor. *Nat. Med.* **2003**, *9*, 669–676. (b) Carmeliet, P. Angiogenesis in life, disease, and medicine. *Nature* **2005**, *438*, 932–936. (c) Carmeliet, P. Angiogenesis in health and disease. *Nat. Med.* **2003**, *9*, 653–660. (d) Ahmed, S. I.; Thomas, A. L.; Steward, W. P. Vascular endothelial growth factor (VEGF) inhibition by small molecules. *J. Chemother.* **2004**, *16*, 59–63. (e) Paz, K.; Zhenping, Z. Development of angiogenesis inhibitors to vascular endothelial growth factor receptor 2. Current status and future perspective. *Front. Biosci.* **2005**, *10*, 1415–1439.

(27) For example, see ref 13d.

(28) (a) For examples, see Tamayo, N.; Liao, L.; Goldberg, M.; Powers, D.; Tudor, Y.-Y.; Yu, V.; Wong, L. M.; Henkle, B.; Middleton, S.; Syed, R.; Harvey, T.; Jang, G.; Hungate, R.; Dominguez, C. Design and synthesis of potent pyridazine inhibitors of p38 MAP kinase. *Bioorg. Med. Chem. Lett.* **2005**, *15*, 2409–2413. (b) For examples, see Pargellis, C.; Tong, L.; Churchill, L.; Cirillo, P. F.; Gilmore, T.; Graham, A. G.; Grob, P. M.; Hickey, E. R.; Moss, N.; Pav, S.; Regan, J. Inhibition of p38 MAP kinase by utilizing a novel allosteric binding site. *Nat. Struct. Biol.* **2002**, *9*, 268–272.

(29) (a) Wang, Z.; Harkins, P. C.; Ulevitch, R. J.; Han, J.; Cobb, M. H.; Goldsmith, E. J. The structure of mitogen-activated protein kinase p38 at 2.1-Å resolution. *Proc. Natl. Acad. Sci. U.S.A.* **1997**, *94*, 2327–2332. (b) Wilson, K. P.; Fitzgibbon, M. J.; Caron, P. R.; Griffith, J. P.; Chen, W.; McCaffrey, P. G.; Chambers, S. P.; Su, M. S. Crystal structure of p38 mitogen-activated protein kinase. *J. Biol. Chem.* **1996**, *271*, 27696–27700.

(30) All kinases were tested at their apparent $K_m$ of ATP with respect to 1 μM of peptide substrate.

(31) Harmange, J. C.; Booker, S.; Buchanan, J. L.; Chaffee, S.; Novak, P. M.; van der Plas, S.; Zhu, X. (Amgen, Inc.) 2,4-Disubstituted pyrimidinyl derivatives for use as anticancer agents. WO 03018021, 2003.

JM701095M